CARDIFF UNIVERSITY
PRIFYSGOL CAERDYDD

ORCA – Online Research @ Cardiff

This is an Open Access document downloaded from ORCA, Cardiff University's institutional repository:https://orca.cardiff.ac.uk/id/eprint/158342/

This is the author's version of a work that was submitted to / accepted for publication.

Citation for final published version:

Maier, W. D. , Wade, B., Barnes, Sarah-Jane and Dutch, R. 2023. Petrogenesis of the Kalka, Ewarara and Gosse Pile layered intrusions, Musgrave Province, South Australia, and implications for magmatic sulfide prospectivity. Australian Journal of Earth Sciences 70 (4) , pp. 453-475. 10.1080/08120099.2023.2173292

Publishers page: http://dx.doi.org/10.1080/08120099.2023.2173292

Please note:
Changes made as a result of publishing processes such as copy-editing, formatting and page numbers may not be reflected in this version. For the definitive version of this publication, please refer to the published source. You are advised to consult the publisher's version if you wish to cite this paper.

This version is being made available in accordance with publisher policies. See http://orca.cf.ac.uk/policies.html for usage policies. Copyright and moral rights for publications made available in ORCA are retained by the copyright holders.

Petrogenesis of the Kalka, Ewarara and Gosse Pile layered intrusions, Musgrave Province, South Australia, and implications for magmatic sulfide prospectivity

WD Maier, School of Earth and Environmental Sciences, Cardiff University, UK

B Wade, Adelaide Microscopy, The University of Adelaide, Australia

Sarah-Jane Barnes, Sciences de la Terre, Université du Québec à Chicoutimi, Canada

R Dutch[a,b,*, a]Geological Survey of South Australia, Department for Energy and Mining, Australia. [b] Department of Earth Sciences, University of Adelaide, Adelaide, SA 5005, Australia.

* Now at Datarock Pty Ltd, Australia

Abstract

The Musgrave Province of central Australia was the focus of long-lived mantle upwelling producing large volumes of magnesian basaltic to tholeiitic magma and their felsic derivatives. The Musgrave Province contains one of the greatest concentrations of mafic-ultramafic layered intrusions globally, grouped as the Giles intrusions. In the present paper we study the magmatic ore potential of the Kalka, Gosse Pile and Ewarara layered intrusions located in South Australia. Ewarara and Gosse Pile appear to have relatively low potential for PGE reefs and magmatic Ni-Cu, based on lack of evident metal enrichment and the absence of a mafic-ultramafic transition zone that hosts most PGE reefs globally. However, mafic ultramafic pipes within the intrusions that could have higher potential have not been studied by us. At Kalka, the mafic-ultramafic transition interval is exposed, rendering this intrusion potentially more prospective for PGE reefs. However, based on the available data

this zone appears to be barren. Instead, there are signs of PGE enrichment and metal ratio variation in the magnetite bearing upper portion of the intrusion suggestive of undiscovered PGE reefs. This interpretation is consistent with subtle metal enrichment of soils adjacent to the upper portion of the intrusion.

Introduction

The Musgrave Province of central Australia contains more than 20 layered mafic-ultramafic intrusions, emplaced at c. 1090 to 1040 Ma (Fig. 1). Forming part of the Warakurna Large Igneous Province (Wingate et al., 2004), the intrusions constitute one of the most important clusters of mafic–ultramafic layered intrusions globally. They have been referred to as the Giles Complex (Daniels, 1974) or the Giles intrusions (Smithies et al., 2009). The prospectivity of the intrusions for magmatic ore deposits remains incompletely understood. This is partly due to sparse exposure and because much of the study area forms part of the Ngaanyatjarra – Anangu Pitjantjatjara – Yankunytjatjara Central Reserve into which access is strictly regulated. To assess the magmatic PGE-Ni-Cu sulfide prospectivity of the intrusions, here we present data on platinum-group and lithophile element contents, as well as Nd and Sr isotope data from the Kalka, Gosse Pile and Ewarara intrusions in South Australia.

Regional geology

The Musgrave Province consists of high-grade metamorphic rocks covering an area of approximately 120 000 km^2 in central Australia (Fig. 1a). It lies at the junction between the North, South and West Australian Cratons amalgamated prior to the Musgrave Orogeny at c. 1220 Ma (Giles et al., 2004; Betts and Giles, 2006; Cawood and Korsch, 2008; Smithies et al., 2010, 2011; Kirkland et al., 2013; Pollett et al., 2019; Donnellan et al. 2019; Goscombe et

al. 2020). The following brief summary of the tectonic evolution is largely based on Maier et al. (2015).

The Province is tectonically bound by the Neoproterozoic to Paleozoic sedimentary rocks of the Amadeus Basin in the north and the Officer Basin in the south (Edgoose et al., 2004). The oldest exposed rocks of the Musgrave Province belong to the undifferentiated **Birksgate Complex** (Major and Connor, 1993). This unit consists of amphibolite to granulite facies, felsic and minor mafic gneisses with igneous, volcanic, volcaniclastic and, less commonly, sedimentary precursors (Edgoose et al., 2004, Wade et al., 2006, Dutch et al., 2013). Igneous protoliths typically have calc-alkaline affinities and trace element tectonic discrimination plots as well as juvenile isotopic compositions suggest the protoliths to the Birksgate Complex formed in a volcanic arc setting (Wade et al., 2006, Dutch et al., 2013). In the eastern parts of the province, these units have been dated to between 1665-1564 Ma (Jagodzinski and Dutch, 2013), with a single age reported as old as c. 1690 Ma (Smits et al., 2014). In the central Musgrave Province, similar lithologies mapped as Birksgate Complex have been dated between 1590-1555 Ma (summarised in Edgoose et al., 2004). In the west Musgrave Province the basement is poorly exposed except for the 1604-1542 Ma Warlawurru Supersuite exposed within a thrust slice near Wannan and on the AGNES map sheet near the SA border. The 1402 Ma Papulankutja Supersuite is also exposed, on the HOLT map sheet (De Gromard and Howard 2019).

Following the formation of the Birksgate Complex units is the **Mount West Orogeny**. This event is only recognised in the western Musgrave Province and is characterized by emplacement of calc-alkaline granites of the Wankanki Supersuite mainly within the central and southeastern part of the west Musgrave Province (Evins et al., 2009; Smithies et al.,

2009). Crystallization ages cluster between c. 1326 and 1312 Ma (Gray, 1971; Sun et al., 1996; White et al., 1999; Bodorkos et al., 2008a–e; Kirkland et al., 2008a–f; Smithies et al., 2009). The rocks are typically metaluminous, calcic to calc-alkaline granodiorites and monzogranites, compositionally resembling Phanerozoic granites of the Andean continental arc (Smithies et al., 2010). Although this event likely extends to the southeastern part of the Musgrave Province, the paucity of geochronology results in the latter domain renders correlations speculative. The Mount West Orogeny may have been triggered by the amalgamation of the North, West, and South Australian Cratons and associated subduction and accretion (Giles et al., 2004; Betts and Giles, 2006; Smithies et al., 2010, 2011; Kirkland et al., 2013).

The 1220–1140 Ma **Musgrave Orogeny** formed in an intracratonic (Wade et al., 2008; Smithies et al., 2009, 2010) or back-arc setting (Smithies et al., 2013). Deformation and high-grade metamorphism resulted in abundant mylonites. The main magmatic components are charnockitic and rapakivi granites of the Pitjantjatjara Supersuite. The earliest Pitjantjatjara granites are interpreted to have formed through deep-crustal melting in the presence of garnet. A transition to granites derived from shallower depth is diachronous, attributed to removal of the lower crust and mantle lithosphere, previously thickened during the Mount West Orogeny (Smithies et al., 2010, 2011). Intrusion of the Pitjantjatjara granites coincided with a 70–100 m.y. period of regional ultra-high-temperature (UHT) metamorphism (King, 2008; Kelsey et al., 2009, 2010; Smithies et al., 2010, 2011; Jagodzinski and Dutch 2013; Tucker et al., 2015), characterized by lower to mid-crustal temperatures of >1000°C, along a geothermal gradient of ≥35–40°C/km. Such conditions are consistent with removal of the lithospheric mantle.

The c. 1090 to 1040 Ma **Giles Event** was characterized by voluminous mafic to felsic magmatism (Fig. 1), including the layered mafic-ultramafic 'Giles intrusions' (G1), massive gabbro (G2) locally mixed and mingled with granite, various dyke suites including the Alcurra Dolerite suite, granite plutons, as well as mafic and felsic lavas, volcaniclastic and sedimentary rocks forming the Bentley Supergroup. All these components are grouped into the Warakurna Supersuite interpreted to have accumulated in the long-lived intracontinental Ngaanyatjarra Rift (Evins et al., 2010b; Aitken et al., 2013). Based in part on the extensive outcrop of the Warakurna Supersuite across ~ 1.5 million km^2 the Giles magmatism has been interpreted as the result of a mantle plume (Wingate et al., 2004; Morris and Pirajno, 2005). However, the most conservative estimates for the duration of mantle magmatism are >30 m.y. with a likelihood it continued for significantly longer (Smithies et al., 2015), with no time-progressive geographical trend or track, inconsistent with a simple plume model (Smithies et al., 2013, 2015; Evins et al., 2010a,b).

Younger events include the 580–530 Ma intracratonic Petermann Orogeny, during which the Proterozoic Musgrave Province units were exhumed and many of the Giles intrusions were fragmented. Additional younger events are reflected by several regional dolerite dyke suites (at c. 1000, c. 825, and c. 750 Ma) and low-volume felsic magmatism (at c. 995 Ma and c. 625 Ma)(Howard et al., 2015).

The Giles intrusions

Important early contributions on the geology of the Giles intrusions include the papers by Nesbitt and Talbot (1966) who proposed that some of the intrusions are tectonised remnants of an originally much larger body, as well as Moore (1971a,b) and Goode and his collaborators who predominantly worked on the Kalka, Ewarara and Gosse Pile intrusions

(Goode, 1970, 1976a,b, 1977a,b,c, 1978, Goode and Krieg 1967, Goode and Moore 1975, Gray and Goode 1989). The Australian Geological Survey Organisation (now Geoscience Australia) began a large multidisciplinary study of the Musgrave Province in the late 1980s (Glikson, 1995; Glikson et al., 1996) which included the Giles intrusions (Ballhaus and Glikson, 1989, 1995; Ballhaus and Berry, 1991; Clarke et al., 1995; Glikson, 1995). More recent work on the mafic-ultramafic intrusions includes studies by Wade (2006) on Kalka, Ewarara and Gosse Pile, Seat et al. (2007, 2009) and Godel et al. (2011) on the Nebo–Babel Ni–Cu ore deposit, Schwarz and Constable (2007) on the Ngunala intrusion in South Australia, Evins et al. (2010a,b) and Aitken et al (2013) on the structural evolution of the province during the Giles Event, Maier et al. (2014, 2015), Karykowski et al. (2015, 2017), Grguric et al. (2018) and Putzolu et al. (2018) on the West Musgrave intrusions and Joly et al. (2015) on a prospectivity assessment of the region.

The Giles intrusions show considerable variation in size (from a few km^2 to >3000 km^2), depth of emplacement (from sub-volcanic to possibly more than 30 km, Goode and Moore 1975), stratigraphy, as well as style of associated mineral deposits. Maier et al. (2014, 2015) grouped the intrusions by their predominant lithologies. Intrusions with important ultramafic segments of wehrlite, harzburgite, websterite and (olivine) orthopyroxenite include Wingellina Hills, Pirntirri Mulari, the Wart, Gosse Pile and Ewarara (Fig. 1c). Intrusions that are predominantly leucogabbronoritic comprise Hinckley Range, Michael Hills, Latitude Hill, Murray Range, Morgan Range, Cavenagh Range and Saturn. The Blackstone, Jameson-Finlayson, and Bell Rock ranges also belong to this group, but they are now believed to be tectonically segmented portions of an originally single body, named Mantamaru by Maier et al. (2014, 2015). Some of the gabbronoritic intrusions contain pyroxenite layers (e.g., Woodroffe/Mt Caroline, Pirajno et al. 2012). Several contain

troctolitic successions, namely Cavenagh, Morgan, Mantamaru and Kalka. Intrusions that contain both ultramafic and mafic segments are rare, comprising Pirntirri Mulari and Morgan in WA and Kalka and Ngunuala in South Australia. In most intrusions, anorthosite is absent or forms thin, centimetric to decametric layers, but Ngunala and Kalka have anorthosites reaching thicknesses of several tens of metres, and one intrusion (Teizi) consists predominantly of anorthosite.

Several of the Giles intrusions contain deposits of magmatic sulfides and oxides. Amongst the former are Nebo Babel (Ni-Cu, Seat et al., 2009), Succoth (Grguric et al. 2018), Manchego (Karykowski et al. 2015) and Halleys (Maier et al. 2015). Wingellina Hills contain PGE reefs with up to several ppm PGE over several thicknesses, and Pirntirri Mulari may also host PGE reefs (Maier et al. 2015). Wingellina Hills contains a world-class Ni laterite deposit with resources of 183 Mt at ~1% Ni and 0.07% Co, with 1.8 Mt of contained metal (Metals X Ltd; http://metalsx.com.au/operations/wingellina_nickel/. (Putzolu et al. 2019). Vanadiferous magnetite occurs at Jameson (Daniels 1974, Maier et al. 2015, Karykowski et al. 2015) as well as in deep portions of Bell Rock intersected by drill core (Pascoe 2012). The latter also contain elevated apatite.

Because the present paper focusses on the Ewarara, Gosse Pile and Kalka intrusions they are described in more detail in the following section. All three intrusions are located close to the Hinckley and Mt.Davies-Numbunja shearzones (Fig. 2).

Ewarara is a relatively small intrusion (stratigraphic thickness ~ 0.5-1.5 km, strike ~ 6 km) (Fig. 3a) emplaced into gneiss of the Birksgate Complex. It is located to the N of the Mt.Davies-Numbunja fault. The intrusion is surrounded by a contact metamorphic aureole, and the felsic host gneisses are sheared at the contact, suggesting intrusion along a pre-

existing shallow-dipping fault (Goode 2002). The layering dips at relatively shallow angle (20°) to the S but steepens in the SE where a possible feeder zone has been inferred (Moore, 1971).

The stratigraphy of the intrusion has been originally established by Moore (1971). At the base of the intrusion is a relatively thin (few centimeters), fine grained, olivine gabbronorite considered to be the only preserved primary magmatic contact amongst the Giles intrusions (Goode 2002). The rocks contain thin felsic xenoliths and elevated biotite suggestive of contamination, and plagioclase laths have a composition of An 66. The contact rocks are overlain by several 100 m of olivine-orthopyroxenite (the Olivine Bronzitite Zone of Goode 1970), consisting of 20-40 % olivine (Fo86-88), 50-70 % orthopyroxene (En89), up to ~5 % plagioclase (~An30) and 5-10 % clinopyroxene, as well as traces of spinel and apatite. The proportions of biotite, ilmenite, magnetite and trace sulfides decrease with height, interpreted to reflect decreasing contamination with the floor rocks. The olivine-orthopyroxenite is overlain by orthopyroxenite grading upward into websterite, making up the Pyroxenite Zone, containing 50-80 % orthopyroxenite, 10-40 % clinopyroxenite, as well as up to a few % interstitial plagioclase (sample 125 has ~5%). At the base of this zone occurs inch-scale layering (Fig. 19 in Goode 2002).

Mineral compositional data were published by Moore (1967, 1971) and Goode and Moore (1975). The latter authors presented microprobe results of one sample having orthopyroxene with Mg# 82.2 and Al_2O_3 4.26 % (Cr not available), and clinopyroxene with Mg# 83.3 and Al_2O_3 4.85 %.

Ewarara (as well as Kalka) contains a number of mafic-ultramafic olivine rich plug-like bodies, forming part of a group of at least 16 bodies intrusive into both granulites and Giles

intrusions, as suggested by lack of deformation and recrystallisation as well as sharp contacts with the country rocks. The plugs are generally up to 100-1000 m across and may contain doleritic chilled margins. Several types have been distinguished. A peridotite group comprises dunites, lherzolites, harzburgites and peridotites with cumulus olivine (Fo87-90) and minor chrome spinel with interstitial pyroxenes, plagioclase, hornblende and biotite. A Picrite group contains 50-65 % cumulus semi-dendritic olivine (Fo82-85) enclosed by poikilitic pyroxene and plagioclase. In addition there are olivine mesogabbros, olivine leucogabbros and leucogabbros.

Gosse Pile is located between the Hinckley and Mt.Davies-Numbunja faults, 10 km towards the E and along strike from Kalka. The body is ~2000 m thick and has a strike length of ~8 km (Fig. 3b). It consists predominantly of steeply S-dipping (45-90°) layers of orthopyroxenite, with minor websterite, peridotite and gabbronorite (Moore 1971a,b; Wade 2006). The rocks contain rare chromite, spinel, hornblende, biotite and sulfides, the latter found only in olivine-pyroxenites.

The rocks are least deformed in the N (where the most magmatic textures of all 3 intrusions occur), whereas along the southern contact deformed pyroxenites with mosaic textures occur indicating movement along the Mount Davies-Numbunja shear zone, a 10 m wide fault that is an offshoot of the Hinckley shear zone and separates Gosse Pile from Mt Davies. The contacts to the gneissic country rocks of the Birksgate Complex are not exposed.

The central and NE parts of the intrusion consist of well layered ultramafic cyclic units, including serpentinite, grading into “picrite” (Moore 1971), possibly representing olivine-pyroxenites. The latter may contain well-laminated xenoliths of orthopyroxenite. In the S, there are interlayered pyroxenites and norites, which led Moore (1971) to propose that this

is the stratigraphic top of the body. Moore considered Gosse Pile to be the lower portion of an originally larger body that included Kalka.

In addition to the layered sequence, Moore (1971) identified 2 types of interpreted late-stage rocks. Along the northern margin occur numerous outcrops of norite containing xenoliths of acid granulite, interpreted to be transgressive relative to the pyroxenites. Associated with the norites are basic pegmatites. In the centre of the intrusion is a gabbroic to noritic layer (the "gabbro band") that is in places anorthositic (i.e., consisting of plagioclase with intercumulus orthopyroxene and clinopyroxene). The gabbro band forms lens-like extensions into the websterite to the N, and may contain irregular blocks of websterite, which led Moore (1971) to propose that it intruded at a relatively late stage, analogous to the transgressive norite. As thus, it may have a similar origin as some anorthosite layers in the Bushveld Complex (Maier et al. 2016).

Initial studies on mineral chemistry were conducted by Goode (1970), Moore (1971) and Goode and Moore (1975). The authors reported that orthopyroxene has Mg# 85.8-77.9, Al2O3 2.56-4.01 %, and Cr 2200-6500 ppm. Clinopyroxene has Mg# 87.6-82.5, Cr 2700-9000 ppm and Al2O3 3.52-6.1 %. No olivine or plagioclase data are available for this intrusion.

The ***Kalka*** intrusion forms a prominent massif (Appendix 1, 2). It has a stratigraphic thickness of ~5000 m, with a strike length of ~10 km (Fig. 3c). Amongst the Giles intrusions it is the one with the broadest compositional range. At its base are relatively unevolved orthopyroxenite and melanorite. In the centre there are thick intervals of (ol)gabbronorite encompassing layers of peridotite. At the top of the intrusion are magnetite-bearing leucogabbronorite, leucotroctolite and anorthosite (Goode 1970; Gray et al. 1981; Glickson et al. 1996, Wade 2006). Kalka is bounded by major faults on all sides. Layering is steeply dipping or locally overturned, attributed to movement along the Hinckley shear zone

(Glickson et al. 1996). The available lithological and petrological data all suggest younging towards the South. The following summary is largely based on Goode (1970).

At the base of the intrusion is a deformed 0.1-0.5 m zone of fine grained gabbronoritic rocks containing hornblende, biotite and opaques as well as felsic lenses and veins. These were interpreted to represent a chilled, contaminated contact phase by Goode (1970). The contact rocks grade into coarser grained cumulates over distances of a few dm to ~1m.

The Pyroxenite Zone (PZ) has a maximum thickness of 450 m and consists mainly of medium- to coarse grained orthopyroxenite or melanorite giving way to websterites with height. Layering is largely caused by modal variation, visible mainly in weathered outcrops. In some cases, layering may be of tectonic origin. The rocks typically show a weak planar lamination consisting of 55-90 % orthopyroxene (grain size 3-4 mm), 5-25 % clinopyroxene (grain size ~2 mm) and 5-10 % interstitial plagioclase (0.5-1 mm). Biotite and other accessories are rare.

The overlying Gabbronorite Zone (GZ) was termed Norite Zone by Goode (1970) but our whole rock data indicate that clinopyroxene constitutes > 10% of the pyroxenes in all analysed samples. The contact between the PZ and the GZ is gradational over a relatively short distance. This zone makes up the bulk of the intrusion, with a maximum thickness of ~3500 m. This zone. Following Goode (1970) the zone is sub-divided into 3 sub-zones. The lower sub-zone (1500-2000 m) consists mainly of gabbronorite with less abundant gabbro, anorthosite and olivine gabbronorite, as well as occasional thin layers of peridotite having the least evolved olivine in the intrusion (Fo87). Layering is locally prominent, occurring at scales of a few centimetres to 100s of metres. However, much of the sub-zone is of a massive character. Planar lamination of pyroxenes and plagioclase is common. Locally,

254 layers are truncating each other and may form scour channels. The middle sub-zone has a
255 similar composition as the basal subzone but is somewhat enriched in oxides (magnetite
256 and ilmenite) and biotite. The sub-zone also contains two laterally extensive, bifurcating
257 granulite slivers, separated by up to 250 m of gabbronorite. The upper sub-zone starts
258 above the upper granulite sliver, is ~500 m thick and consists largely of magnetite-bearing
259 gabbronorite as well as some anorthosites showing small-scale modal layering. The sub-
260 zone contains more olivine than the underlying sub-zones, including, in the South, a layered
261 peridotite member occurring ~ 150 m above the base and traceable for ~2 km along strike.
262 In the North occurs a transgressive magnetite/ilmenite body, 100 m x 20-50 m in width and
263 containing up to 1.28 % V_2O_5. A characteristic of many gabbronorites is the occurrence of
264 rounded and irregular inclusions of plagioclase in orthopyroxene and, to a lesser extent,
265 clinopyroxene, interpreted to represent resorbed remnants of plagioclase grains suspended
266 in the magma.

267 In the central and eastern part of Kalka, the Gabbronorite Zone contains a ~600 m thick
268 interval of relatively olivine rich lithologies termed the Olivine Gabbro Zone (OGZ). It
269 consists of layers of olivine gabbro, locally grading to lherzolite, dunite and clinopyroxenite,
270 that are hosted within gabbronorite (Gray and Goode 1981). Individual layers may show well
271 developed igneous layering at variable scales (inch scale to decametric), typically with sharp
272 contacts. However, layers do not seem to be laterally correlatable. Instead, they are
273 envisaged to represent an “intertongued facies change” (Goode 2002), somewhat analogous
274 to the Pseudoreefs of the Bushveld Complex (Maier and Waters, 1993). At the top of the
275 zone is an intermittently developed ~5 m rhythmic layered unit, termed the Johnson layered
276 unit.

The Anorthosite Zone forms the uppermost portion of the Kalka intrusion. It is up to 800 m thick and consists of locally well-layered anorthositic, leucogabbroic and leucotroctolitic rocks that commonly contain up to ~ 5-10 % magnetite and ilmenite. The base of the zone is defined by the lenticular, 0.5-3 m olivine-magnetite member containing ~40 % interstitial magnetite, olivine (Fo63), ilmenite and green spinel. Additional thin magnetite/ilmenite-rich layers may occur throughout the zone. A characteristic feature of the zone are irregular lenses and schlieren of heteradcumulate troctolite within adcumulate anorthosite termed mottled or clump texture by Goode (1977). In addition, Goode (1970) described sedimentary-like structures including channel-like truncations resembling Bushveld potholes, cross-bedding, load casts, and graded layering (both normal and reversed). Interstitial phases such as Fe oxides, biotite, hornblende and sulfides (mainly pyrrhotite and chalcopyrite) as well as transgressive mafic pegmatites are more common in this Zone than in the underlying zones, albeit still occurring in accessory to minor amounts. In the uppermost portion, rare apatite occurs.

Initial mineral chemistry studies on Kalka olivine and plagioclase were conducted by Goode (1970), using X-ray diffraction. Goode and Moore (1975) reported that Kalka orthopyroxene has Mg# 78-86 with Al_2O_3 1.6-5%. Clinopyroxene has Mg# 72-84. Olivine in the Kalka Olivine Gabbro Zone has Fo70-85, in the lower Norite zone it has up to Fo87, and in the anorthosite zone it has Fo75-60 (Goode 1970, 1976). No data on Ni contents of olivine are available. Gray and Goode (1985) published abundant plagioclase compositional data for a profile across Kalka, showing a broad trend of upward decreasing An contents from ~76 in the Pyroxenite Zone (one sample having An 67) to ~60 at the top of the intrusion. Diversions from this trend include high-An in the Olivine Gabbro Zone (up to An 83) and some samples with up to An 76 in the Anorthosite Zone.

Methods

All samples analysed were from historical samples in the rock crypt of University of Adelaide. The Ewarara traverse samples were collected by ATD Goode and GW Krieg during their honours projects in 1965. The Kalka traverse was collected by ATD Goode during his PhD in 1970, and the Gosse Pile traverse was done by A Moore in 1970, also during his PhD.

After milling the samples in a W-Carbide mill, the concentrations of major and trace elements were determined by ICP-MS at Amdel Laboratories in Adelaide. Mineral compositions were determined at Adelaide University, using an electron microprobe and a Laser ICP-MS (for REE). Thirty eight whole rock samples and 29 mineral separates were analysed for Nd and Sr isotopes (see Wade, 2006, for analytical details). The whole rock data were used to estimate modal proportions of the rocks, being that CIPW norms fail to assign Al to pyroxenes, thereby resulting in overestimation of the proportion of plagioclase.

Platinum-group elements (Ru, Rh, Pd, Os, Ir, Pt) and Au for 49 samples (8 each from Gosse Pile and Ewarara, 33 from Kalka) were determined at LabMaTer, UQAC. The PGE were pre-concentrated by Ni-sulfide fire assay and co-precipitated with Te, followed by analysis by solution inductively coupled plasma – mass spectrometry (ICP-MS) using the method described by Savard et al. (2010). The international reference material (OKUM) from Geo Labs - Ontario was analyzed alongside the samples to monitor data quality. The results obtained for the reference material are consistent with the certificate values (Table 1).

Results

Petrography

Scans of 23 thin sections across the Kalka, Ewarara and Gosse Pile stratigraphy are provided in Appendix 3-5, with selected samples shown in Fig. 4. In all intrusions, low-T alteration is relatively minor, but many of the samples are intensely deformed and recrystallised, showing sub-grains, bent and spindle-shaped twin lamellae and undulous extinction. The rocks have mosaic-porphyroclastic textures, with larger crystals of mainly orthopyroxene set in a finer-grained matrix of plagioclase and pyroxene. Some of the more resistant garnet and orthopyroxene grains are surrounded by fluidal-mosaic domains. Past authors have documented a range of additional features resulting from high grade metamorphism and high-pressure sub-solidus equilibration, including spinel exsolution in pyroxenes and plagioclase, rutile exsolution in pyroxenes, antiperthite exsolution in plagioclase, and orthopyroxene, clinopyroxene and spinel coronas between olivine and plagioclase (Goode and Moore 1975; Ballhaus and Berry 1991; Maier et al. 2015). Textures that appear to be least metamorphic are found in the northern portion of Gosse Pile, distal to the Numbuja fault zone where one can see subhedral olivine and pyroxene, as well as interstitial plagioclase.

Ultramafic rocks at Ewarara and Gosse Pile comprise mostly websterites and orthopyroxenites, the latter mainly at Gosse Pile (Table 2). They mostly contain less than 5% plagioclase. In contrast, most of the analysed samples of the Kalka Pyroxenite Zone are strictly speaking melagabbronorites, as they have around, or just above, 10 % plagioclase (Fig. 4). In addition to the pyroxenites, Kalka has a few layers of (feldspathic) lherzolite, located in the central and upper portion of the intrusion. Most of the ultramafic rocks in all intrusions show mosaic textures in which individual grains are approximately equidimensional (i.e., equant or isometric), have similar size and approximately polygonal shapes and display common kink banding. The porphyroclasts consist predominantly of

346 subhedral oprthopyroxene. Kalka picrites can be coarse grained showing large (~1 cm)
347 clinopyroxene porphyroclats hosting olivine chadacrysts, but some picrites are fine grained
348 (0.1-0.2 mm, e.g., sample 314-200 at 4303 mab).

349 Gabbronorites form the predominant rock type at Kalka whereas at Gosse Pile gabbroic
350 rocks are confined to the relatively thin gabbro band in the centre of the intrusion (samples
351 111-107, Table 2) and the very base of the intrusion (312b). At Ewarara, there are several
352 samples at the top of the intrusion (# 125-121) that have small amounts (typically ~5-10%)
353 of mostly interstitial plagioclase. The gabbronorites tend to be strongly deformed, with
354 plagioclase showing undulous extinction, kink banding, bent and tapered twin lamellae, and
355 sub-grains. Grain boundaries are mostly irregular at Kalka and Ewarara but show less
356 deformation at Gosse Pile. Kalka gabbronorites can be olivine bearing and many plagioclase
357 grains contain abundant small grains of oxides (magnetite and ilmenite).

358 Anorthosites, troctolites and leucogabbros make up the Kalka Anorthosite Zone. The rocks
359 are mostly distinctly foliated. Troctolites have 15-20 % olivine and small amounts of
360 clinopyroxene and orthopyroxene, the remainder being plagioclase. They are thus classified
361 as leucotroctolites. Within the Anorthosite Zone there also occur some leucogabbros,
362 having 75-80 % plagioclase, 10-20 % clinopyroxene, and small amounts of olivine and
363 orthopyroxene. Olivine is medium grained (up to ~2 mm), anhedral and shows undulous
364 extinction. Only one of our samples is an anorthosite, consisting of > 95 % plagioclase, with
365 the remainder being clinopyroxene.

366 *Mineral chemistry*

367 In the present study, we focus on reporting the major, minor and trace element
368 compositions of plagioclase, orthopyroxene and clinopyroxene in 11 samples (four samples

from Kalka, four samples from Ewarara and three samples from Gosse Pile), originally presented in Wade (2006). Microprobe analyses indicate that orthopyroxene from the four Kalka samples has Mg# up to 81-76, the three Gosse Pile samples have Mg# 88-83, and the four Ewarara samples have Mg# 87-82. All orthopyroxenes have relatively high Al_2O_3 (2.65 % at Kalka, 3.56 % at Ewarara and 3.58 % at Gosse Pile). Kalka orthopyroxene has 0.1-0.23 % Cr_2O_3, whereas Ewarara and Gosse Pile have notably high Cr_2O_3 contents reaching 0.83 and 0.71 wt%, respectively. Kalka clinopyroxenes have Mg# 85-76, Al_2O_3 2.9-5.7 wt%, Cr 140-3400 ppm, Gosse Pile clinopyroxene has Mg# 88-85, Al_2O_3 4.3-4.7 wt%, Cr 4690-6600 ppm, and Ewarara clinopyroxene has Mg~ 89-87, Al_20_3 4.7-5.1 wt%, Cr 9500-3400 ppm. Plagioclase at Kalka has An 0.75-0.82, Gosse Pile has 0.72-0.78, and Ewarara 0.69-0.47.

Laser ablation ICP-MS data show that clinopyroxene, orthopyroxene and plagioclase from Kalka and Ewarara are generally richer in incompatible trace elements (ITE) than those from Gosse Pile. REE patterns are shown in Fig. 5 and a broader range of ITE patterns (for clinopyroxene) are shown in Fig. 6. The trace element patterns for clinopyroxene and orthopyroxene are sloped towards low LREE contents, reflecting the relatively low D of the LREE with regard to pyroxene. At Kalka and Ewarara the basal samples have higher ITE (including REE) contents and more fractionated patterns than the other samples, for both pyroxenes and plagioclase. At Gosse Pile, the trend is reversed, with the interpreted basal sample (Moore 1971, Wade 2006) having the lowest ITE and REE contents. In all three intrusions, clinopyroxene is characterised by negative Nb-Ta and Ti anomalies (Fig. 6).

Lithophile major and trace element geochemistry

Binary variation diagrams of the lithophile major and trace elements (Fig. 7) confirm that the three intrusions consist of varying proportions of orthopyroxene, clinopyroxene,

392 plagioclase and olivine. The CaO/Al_2O_3 plot (Fig. 7a) shows that most samples from Ewarara
393 and Gosse Pile are ultramafic in the sense of Streckeisen (1974), i.e., containing > 90 % mafic
394 minerals. The ultramafic rocks at Kalka comprise three samples of the Pyroxenite Zone, one
395 sample from the Olivine Gabbro Zone, and two samples from the Peridotite Member in the
396 upper Gabbronorite sub-zone.

397 Most of the analysed pyroxenites are websterites, except for several of the Gosse Pile and
398 Ewarara pyroxenites which are orthopyroxenites (i.e., having a ratio of orthopyroxene to
399 clinopyroxene of > 9). There are no clinopyroxenites amongst our samples, but isolated
400 layers of clinopyroxenite were mentioned for all intrusions in Goode (1970). The mafic rocks
401 are mostly (ol)gabbronorites having variable ratios of plagioclase to pyroxene (but clustering
402 around the cotectic ratio of ~60:40, Fig. 7b) and orthopyroxene to clinopyroxene. Olivine is
403 mostly absent, except for some Kalka gabbronorites. The Kalka troctolites within the
404 Anorthosite Zone contain 10-20 % olivine, 70-80 % plagioclase and minor pyroxene. One
405 sample is an almost monomineralic anorthosite.

406 The rocks have up to 7000 ppm Cr which can largely be accounted for by orthopyroxene and
407 clinopyroxene (Fig. 7c), i.e., there is little or no chromite (see also Goode 1970). Nickel
408 contents are up to 1300 ppm and, based on a good positive correlation with MgO, appear to
409 be largely controlled by the silicate minerals (Fig. 7d).

410 The Sr contents of the rocks are between 400 ppm in anorthosite and 10 ppm in some
411 Gosse Pile orthopyroxenites, consistent with the low plagioclase contents of these
412 ultramafic rocks (Fig. 7f). In contrast, the orthopyroxenites/melanorites of the Kalka
413 Pyroxenite Zone have up to 60 ppm Sr, reflecting their relatively high plagioclase contents.

The K_2O contents of the intrusions show a general trend of low concentrations in the ultramafic rocks and higher values in the mafic rocks (up to ~0.2% K_2O, Fig. 7e). Three of the ultramafic samples, occurring at the base of Kalka and Ewarara, have somewhat higher K_2O contents than the other samples. In addition, there are several Kalka gabbronorites that are markedly enriched in K_2O (and other ITE). These come from the interval overlying the granulite slivers in the centre of the intrusion. Th (Fig. 7g) and Nd (Fig. 7h) show very similar trends to K_2O, with enrichments seen above the granulite slivers.

The variation in the concentration of lithophile elements at Kalka are plotted vs stratigraphic height in Fig. 8. MgO varies from ~20 wt.% in the websterites and melagabbronorites of the Pyroxenite Zone to ~10 wt.% in most gabbronorites of the Gabbronorite Zone and the troctolites of the Anorthosite Zone. Particularly high MgO (up to 30 wt.%) is found in several peridotitic layers within the Olivine Gabbro Zone as well as the Peridotite Member of the upper Gabbronorite Zone. Al_2O_3 shows low values (<10 wt.%) in the basal websterites and melagabbronorites, and higher (~20 wt.%), yet upward decreasing values in the Gabbronorite Zone, reflecting decreasing An content of plagioclase with height. The highest Al_2O_3 contents occur in the Anorthosite Zone. Ni and Cr both show broad upward decreasing concentration, consistent with their compatibility into olivine and pyroxene. Progressive differentiation of the intrusion is also reflected in upward decreasing whole rock Mg# (from ~0.8 at the base to ~0.3 near the top). In contrast, An content of plagioclase (calculated from whole rock data and using microprobe data of Gray and Goode 1989) shows a less regular trend, varying from ~80 to ~60, but with several reversals, including in the Olivine Gabbronorite Zone, the Peridotite Member, and at the base of the Anorthosite Zone.

436 The incompatible element K_2O shows no systematic increase with height (although the
437 ultramafic rocks tend to have lower incompatible trace (ITE) element contents). In contrast,
438 Nd and Th show subtle trends of upward decreasing concentration, suggesting that ITE
439 contents are partially controlled by the trapped melt and/or contamination of the magmas,
440 as further explored in a subsequent section. Vanadium shows a complex trend, being
441 relatively elevated in the basal websterites, sharply lower the lowermost samples of the
442 Gabbronorite Zone, and from then on increasing with height to peak near the top of the
443 Gabbronorite Zone (~300 ppm). Our samples from the Anorthosite Zone have low V
444 contents, possibly due to scavenging of V by cumulus magnetite forming in the Olivine-
445 Magnetite Member at the base of the Anorthosite Zone which has not been sampled and
446 analysed for this study.

447 Compositional variation with stratigraphic height for Ewarara and Gosse Pile are shown in
448 Appendix 6 and 7. Both intrusions show much less systematic variation than Kalka as
449 reflected by relatively constant Mg#, except for relatively lower values at the base and the
450 top. Gosse Pile shows minor metal enrichment at the base, and upward decreasing Cu
451 content. Cu/PGE is relatively high at the base, possibly in response to localised sulfide
452 saturation. Pd/Ir is also relatively high, perhaps due to some Pt+Pd mobility in floor derived
453 fluids.

454 Ewarara also shows (minor) metal enrichment at the base, and upward decreasing Cu.
455 Cu/PGE is at the level of PM throughout, thus there is little evidence for sulfide segregation.
456 Pd/Ir is relatively low throughout.

457 *Chalcophile element geochemistry*

458 The bulk of the rocks from the analysed intrusions have < 50 ppm Cu and <20 ppb Pt+Pd
459 (Fig. 9), without significant systematic variation between mafic and ultramafic rocks. These
460 samples could conceivably have crystallised from S undersaturated magmas. The main
461 exceptions are a relatively small group of gabbronoritic and troctolitic samples that have Cu
462 contents of up to 250 ppm and Pt+Pd contents of up to 200 ppb. Cu/Pt+Pd is mostly around
463 the level of primitive mantle (~2500). Significantly higher values, indicative of PGE depletion,
464 occur in a few ultramafic rocks from Gosse Pile and in a number of gabbronoritic and
465 troctolitic Kalka samples located above the granulite slivers, as further discussed below.
466 Values significantly below PM (ie indicating the presence of PGE rich sulfides) are also
467 largely confined the hanging wall of the granulite slivers. Pd/Ir is mostly 1-4 at Ewarara and
468 Gosse Pile, whereas Kalka shows more variation; The basal websterites have the lowest
469 Pd/Ir of all analysed samples, whereas the gabbronorites have Pd/Ir up to ~ 60.

470 For the Kalka intrusion, chalcophile elements are plotted vs height in Fig. 10. The most
471 notable trend is that chalcophile elements are generally low in the rocks below the granulite
472 slivers, whereas they are markedly elevated, albeit with significant scatter, in the upper
473 gabbronorite sub-zone above the slivers. The Anorthosite Zone is strongly depleted in PGE
474 and Au, although Cu contents may be relatively high (at up to ~100 ppm). Notably, the peak
475 levels of the various chalcophile elements show a certain offset pattern in that Ir and Ru
476 peak first (at a height of ~2500 m), followed by Rh (at ~3450 m), Pd (at ~ 3650 m), and then
477 Pt and Au (at ~4300 m).

478 Cu/Pd is mostly around PM level below the granulite slivers, but significantly below PM in
479 the first two samples above the granulite slivers. There is strong scatter in the uppermost
480 portion of the Gabbronorite Zone, and generally high values (above PM) occur in the

Anorthosite Zone. Pt/Pd is mostly > 1, and Pd/Ir shows a broad trend of increasing values with height, from ~1 to ~100, consistent with progressive differentiation of the magma.

Spider patterns (Appendix 8) show that few of the Kalka rocks (nor Gosse Pile or Ewarara) are PGE depleted, except the Anorthosite Zone, consistent with highest reef prospectivity possibly below the Anorthosite Zone. Kalka rocks tend to become more fractionated with height, with the exception of OGN.

Nd and Sr Isotopes

The analysed intrusions show contrasting trends in Nd and Sr isotopes plotted vs stratigraphic height. The Kalka samples show a relatively enriched component at the base which is overlain by progressively less enriched rocks with height, except for a reversal in εNd in the centre of the intrusion. The Ewarara intrusion shows relatively homogenous εNd and εSr throughout, comparable to the values found in the upper portion of Kalka. Gosse Pile shows an inverse trend to Kalka, with relatively unenriched signatures at the interpreted base, and a progressively more enriched signature, resembling that of the base of Kalka, in the interpreted upper portion.

Discussion

Nature of parent magmas to the intrusions

Knowledge of the composition of the parent magma(s) of an intrusion is important to constrain the nature of the mantle source of the magma, the degree of crustal contamination, the crystallization history of an intrusion, and thus ultimately the prospectivity for magmatic ore deposits.

Godel et al. (2011) have studied a suite of dykes in the Nebo-Babel area and argued that the most likely parent magma to the Giles intrusions is a Ti-depleted high magnesian basalt termed NB1. They used MELTS modelling to show that at a pressure of 3.5 kbar this magma has a crystallization order of olivine > olivine+ clinopyroxene > chromite+ clinopyroxene+ plagioclase, consistent with the present intrusions and most other Giles intrusions (Ballhaus et al. 1995; Maier et al., 2015).

Crustal contamination of the magmas

The studied intrusions have εNd mostly from -1 to –5 and εSr 20-80 ($^{87/86}Sr_i$ 0.704-0.709) (Fig. 11,12). These relatively enriched signatures could be explained by variable crustal contamination, or melting of compositionally diverse mantle sources, or both. In situ crustal contamination is consistent with the presence of the lowest εNd and highest εSr in the basal rocks of Kalka, as well as field evidence such as the presence of xenoliths and rheomorphic felsic veins as well as the predominance of orthopyroxene over clinopyroxene, and the absence of olivine, near the base of some intrusions (e.g., Wingellina Hills, Kalka). The basal rocks at Kalka also show an enrichment in ITE in pyroxene (Fig. 5 & 6). A further horizon of enhanced crustal component at Kalka is the interval overlying the central granulite slivers where whole rock ITE contents (and PGE) show a marked increase. Interestingly, Nd isotopes are decoupled from this increase, peaking instead below the granulite sliver, for reasons presently not well understood.

In Fig. 12 the available Nd and Sr isotope database of the Giles intrusions are plotted. They show a range of Nd and Sr isotopic signatures, likely resulting from variable crustal contamination. The troctolitic intrusions have relatively unenriched signatures, but the more mafic and ultramafic intrusions, notably Cavenagh, Morgan, Pirntirri Mulari, and

525 Murray, show good overlap with the South Australian intrusions, including the elevated
526 enriched component at the base of Kalka which matches that observed at Cavenagh.

527 The nature of the contaminant at Kalka and other Giles intrusions remains debated. Most
528 Musgrave crustal rocks have εNd values not lower than -6 (Maier et al. 2015). To explain
529 εNd values as low as -5 in the intrusives, this would require an unrealistically high degree of
530 contamination of the magma. However, granites of the regionally occurring Pitjantjatjara
531 Supersuite are extremely rich in HFSE, which may greatly reduce the required amounts of
532 contamination (Kirkland et al., 2013). Isotopic data for the troctolitic intrusions (namely
533 Mantamaru) approximate the chondritic uniform reservoir (CHUR) (εNd mostly from 0 to +2,
534 $^{87/86}Sr_i$ ~ 0.704), i.e. markedly higher εNd and lower $^{87/86}Sr_i$ than any Musgrave crust present
535 at the time. These data suggest minor (<5%) crustal contamination in most troctolitic Giles
536 intrusions, and slightly higher for Kalka (Maier et al. 2015, and Fig. 12). This interpretation is
537 consistent with the less pronounced negative Nb and Ti anomalies in the studied intrusions
538 compared to the Main Zone of the Bushveld Complex (Fig. 6). Note that the troctolitic upper
539 portion at Kalka shows less crustal signature than the basal portions (Fig. 11), although at
540 εNd of -1, it is more enriched than the Western Australian troctolitic intrusives.

541 *Magma emplacement*

542 Field relationships and compositional data indicate that the depth of emplacement of the
543 Giles intrusions varied considerably. Whereas some of the WA intrusions (e.g. Blackstone)
544 were emplaced at shallow, sub-volcanic crustal levels (Maier et al. 2015), some of the
545 ultramafic intrusions were likely emplaced at much greater depth. Based on features such as
546 high Al and Cr concentrations of pyroxene, spinel exsolution in pyroxene and plagioclase,
547 rutile exsolution in pyroxene, antiperthitic exsolution in plagioclase, and orthopyroxene–

548 clinopyroxene–spinel–albite coronas between olivine and plagioclase, Goode and Moore
549 (1975) suggested that the Ewarara intrusion was emplaced at a pressure of 10–12 kbar.
550 Analogous compositional features at Kalka and Gosse Pile suggest a broadly similar
551 emplacement depth. If the thickness of the crust at the end of the Musgrave Orogeny, just
552 40 My before the Giles event, was 35 km (Smithies et al., 2011), the Ewarara intrusion
553 would have intruded near the base of the crust. Ballhaus and Berry (1991) proposed a
554 somewhat shallower emplacement depth of 6.5 kbar (~20 km) for the Wingellina Hills
555 intrusion.

556 Emplacement into relatively deep crustal levels could explain why ultramafic Giles intrusions
557 are less abundant than gabbroic and troctolitic bodies, and why the former are
558 proportionally more abundant in South Australia than in Western Australia - the South
559 Australian crust is exposed at a deeper level (Goode, 2002).

560 Field relationships also allow to place some constraints on emplacement dynamics. For
561 example, the close spatial association of many microgabbros with fragments and schlieren
562 of pyroxenite in several of the WA intrusions suggests a semi-consolidated magma chamber
563 that was frequently replenished by unevolved magma which may have undergone
564 intraplutonic quenching upon emplacement (Goode 1970; Maier et al. 2015).

565 *Comparison of the South Australian intrusions to layered intrusions elsewhere*

566 One way to understand the origin of layered intrusions is to compare them to other, well
567 characterised intrusions. The geology and geochemistry of the Giles intrusions in WA has
568 been re-evaluated by Maier et al. (2015). Their data can be used as a baseline to assess the
569 prospectivity of the three South Australian intrusions studied here. In terms of
570 differentiation state, Gosse Pile and Ewarara are relatively unevolved, overlapping with

571 Pirntirri Mulari, the Wart and Wingellina Hills. Kalka is somewhat more differentiated, with
572 Mg# ranging from #85 to 65.

573 Wingellina Hills is the only Giles intrusion that contains schlieren and lenses of chromitite
574 within peridotite (Ballhaus and Glickson 1989). This is expressed by markedly higher Cr/V
575 than in all other Giles intrusions (Fig. 13). The only other Giles intrusion where chromite is
576 relatively common (although only in disseminated form) is Pirntirri Mullari. Ballhaus and
577 Glickson (1995) suggested that the Giles intrusions have low chromite because they
578 crystallised from a relatively Cr poor parent magma, with local chromite crystallisation
579 triggered by supercooling, but the data of Godel et al. (2011) indicate Cr levels in NB1-2
580 comparable to, e.g., Bushveld magnesian basalt, likely parental to many of the Bushveld
581 massive chromtities. Alternatively, the low chromite content in the Giles intrusions could
582 reflect the fact that in most intrusions cpx preceded opx on the liquidus. As cpx has higher
583 Cr than opx, this could result in early depletion of Cr and suppression of chromite stability.
584 Notably, Wingellina Hills appears to be one of the few Giles intrusions with early
585 crystallisation of opx, as indicated by the presence of a thick harzburgite at its base (Maier
586 et al. 2015), consistent with the idea that early cpx suppresses chromite.

587 The concentrations of Ni, Cu and PGE at Ewarara, Gosse Pile and Kalka overlap with those in
588 the WA Giles intrusions, being generally relatively low (Fig. 14). The only Giles intrusion that
589 shows PGE grades approaching economic levels is Wingellina Hills (Maier et al. 2015). In
590 part, it could reflect underexploration. At Pirntirri Mulari, Maier et al. (2015) have proposed
591 a prospective horizon in the UM-mafic transition zone. This interval remains poorly studied
592 in most Giles intrusions.

593 Kalka has magnetite rich horizons in its upper, gabbronoritic and troctolitic-anorthositic
594 portions, analogous to other fractionated Giles intrusions such as Jameson, Finlayson,
595 Blackstone and Bell Rock. No information is currently available on the V content of the Kalka
596 magnetite.

597 Amongst the best characterised LI on Earth is the Bushveld Complex. It thus makes sense to
598 compare the lithostratigraphy of the intrusions with that of the Bushveld (Fig. 15). Based on
599 indicators such as An of plag, Mg# of pyroxene and whole rock, as well as lithology, Gosse
600 Pile and Ewarara, as well as the lower portions of Pirntirri Mulari, Wingellina Hills and the
601 Wart are stratigraphic analogues of the LZ and LCZ. They have broadly similar olivine
602 compositions and they show basal compositional reversals, thick ultramafic portions, and a
603 number of ultramafic–mafic cyclic units.

604 Morgan, Cavanagh, Hinckley and Blackstone are analogues of the MZ, whereas Jameson as
605 well as the upper portions of Blackstone and Bell Rock are equivalent to the UZ. Of all
606 intrusions, Kalka spans the greatest compositional variation, equivalent to the interval from
607 the Upper CZ across the MZ and into the Upper Zone.

608 The data of Fig. 15 could suggest that some or all of the Giles layered intrusions could be
609 tectonically dismembered remnants of a much larger body (Sprigg and Wilson (1959),
610 Nesbitt and Talbot (1966), Moore (1971), Glikson (1995), Smithies et al. (2009), Howard et
611 al. (2011b), Aitken et al. (2013) and Maier et al. (2015). For example, the ultramafic
612 intrusions located in the Tjuni Purlka Zone (Wingellina Hills, Pirntirri Mulari, The Wart,
613 Morgan Range, Kalka, Gosse Pile, and Ewarara) share certain similarities (notably mineral
614 compositions) and it could be speculated that they originally formed a single body.
615 However, this would imply lateral movement of up to 50 km within the Tjuni Purlka Zone.

Goode (1978) suggested that Gosse Pile represents the lower portion of Kalka, making the combined intrusion ~8000 m thick. The idea was, in part, based on scattered outcrops of ultramafic and mafic rocks extending from Kalka across the Scarface shear zone towards Gosse Pile. Our geochemical data provide no clear answer: Kalka pyroxenites are more Ir and Rh rich (and have lower Pd/Ir, but similar Cu/PGE) than Gosse Pile ultramafic rocks. Gosse Pile has low Pt/Pd whereas Kalka has Pt/Pd at mantle level. Furthermore, Kalka pyroxenes and plagioclase are markedly more enriched in ITE than Gosse Pile. Finally, the basal Kalka sample shows enriched isotopic signature, potentially indicating enhanced in situ contamination of the magma.

To our mind, another open question remains the orientation of Gosse Pile. Moore (1971) suggested that plagioclase-rich (noritic) rocks associated with the highly deformed gneissic pyroxenites in the south of the intrusion represent its fractionated uppermost portions. However, many LI have relatively feldspathic rocks along their basal contacts (e.g., Bushveld, Monchepluton), resulting from contamination and supercooling. One could thus also interpret the Gosse Pile norites as representing the base of the intrusion. This interpretation would be consistent with their isotopically enriched composition, but the question clearly needs more work.

Prospectivity for PGE deposits

In order to assess prospectivity, one needs to have reliable ore formation models. The traditional approach has been comparison to other mineralised intrusions. More recently theoretical modelling has become more important, but that too has remained inconclusive.

Considering comparison to other mineralised intrusions first. In the Bushveld and many other LI on Earth, the main PGE reefs occur in the ultramafic-mafic transition interval. In

addition, sub-economic reefs may occur at the base. In the richest examples of this (Bushveld, Portimo), the internal reefs abut against the floor. These data suggest that Pirntirri Mulari, Wingellina Hills, Wart and Morgan and Kalka are most prospective for PGE reefs. However, there are no changes in Cu/Pd across the ultramafic-mafic transition interval at Kalka. The Wingellina PGE reefs occur in a comparable stratigraphic level, and there are some indications that a similar horizon may exist in the Pirntirri Mulari intrusion. The equivalent prospective horizon of The Wart, Ewarara, and Gosse Pile are not exposed, and the available PGE data (notably the mostly undepleted PGE patterns) give no indication that significant PGE enrichments could have been missed in the ultramafic portions or at the base of the intrusions, even though no samples have been analysed from the (strongly altered) NE hills section of Gosse Pile, a several 100m thick zone forming the most northeasterly, and thus likely lowermost portion of the intrusion. To our knowledge there is no soil sediment data available for areas in the vicinity of Gosse Pile and Ewarara. The soil sediment data from the northern edge of Kalka show no aniomalous values in PGE or Cu, providing no indication for the presence of potential basal sulfide mineralisation (Gum and Constable, 2003).

Another target could be the onset of magnetite. Magnetite-rich upper portions of layered intrusions tend to be PGE mineralised in many intrusions globally (Smith and Maier 2021). Amongst the Giles intrusions, PGE enrichment has been found at Halleys and Jameson (Maier et al. 2015, Karykowski et al. 2016). Kalka shows a clear enrichment in PGE in the relatively magnetite rich upper gabbronorite zone, accompanied by significant variation in Cu/Pd (Fig. 10). Estimated R factors are very high here (approaching 100000, Appendix 9) analogous to the reef intervals of, e.g., the Bushveld Complex. Thus, this represents the key PGE reef target in the intrusion and should be investigated in more detail, as current

sampling density is low. Notably, limited soil geochemical data from the Kalka area indicate a subtle enrichment in Cu and PGE (up to around 6 ppb Pt+Pd) along the western edge of Kalka (Gum and Constable, 2003), broadly coincident with the transition interval between the Gabbronorite and Anorthosite zones and demonstrating that soil geochemical surveys may be useful in detecting PGE reefs. Additional PGE and Cu enrichments in soils occur between Kalka and Mt Davies.

Conclusions

The Musgrave Province was the focus of long-lived mantle upwelling producing large volumes of magnesian basaltic to tholeiitic magma and their felsic derivatives. Magmatism led to crustal melting, lithospheric delamination, and a high crustal heat flux over >200 m.y. The Province contains one of the greatest concentrations of mafic-ultramafic layered intrusions globally, many of them being fragmented due to syn- to post-magmatic tectonism. The degree of crustal contamination was mostly relatively minor (<10%), although locally, basaltic magmas mingled with coeval granitic magmas.

Large mafic-ultramafic magmatic events are believed to result in increased and prolonged heat flux into the crust, potentially triggering crustal melting, devolatization, and large-scale fluid flow. This should theoretically increase the potential for magmatic PGE–Cr–V-Fe–P deposits in the largest intrusions, and Ni–Cu sulfide deposits in dynamic magma feeder conduits or at the base of layered intrusions where contamination is enhanced. Several deposits of this type have been discovered in the Musgrave Province, namely at Nebo Babel (interpreted to be a magma conduit), Wingellina Hills (PGE reefs in a large layered intrusion), as well as contact style deposits at Halleys, Manchego, and Succoth.

In the present study, we examined the magmatic ore potential of the Ewarara, Gosse Pile and Kalka intrusions. Ewarara and Gosse Pile appear to have relatively low potential for PGE reefs and magmatic Ni-Cu, based on lack of evident metal enrichment, the paucity of S in the crustal host rocks, and the absence of a mafic-ultramafic transition zone that typically hosts most PGE reefs globally. However, the mafic-ultramafic pipes located within the two intrusions remain unstudied with regard to metals. They constitute potential targets for both PGE and Ni-Cu. At Kalka, the mafic-ultramafic transition interval is exposed, rendering this intrusion potentially more prospective. However, based on the available data this zone appears to be barren. Instead, there are signs of PGE enrichment and metal ratio variation in the upper portion of the intrusion, namely above the granulite slivers and in the magnetite bearing upper Gabbronorite Zone, possibly triggered by Fe loss of the magma.

Acknowledgements

We acknowledge the Anangu Pitantjatjara Yankuntjatjara peoples and appreciate their support of the previous research and sampling undertaken by the researchers whose samples have been used in this study.

References

Aitken, A.R., Dentith, M.C., Evans, S.F., Gallardo, L.A., Joly, A., Thiel, S., Smithies, R.H. & Tyler, I.M. (2013). *Imaging crustal structure in the west Musgrave Province from magnetotelluric and potential field data.* Geological Survey of Western Australia. Report 114, 81p.

Ballhaus, C. & Berry, R.F. (1991). Crystallization pressure and cooling history of the Giles Layered Igneous Complex, central Australia. *Journal of Petrology*, 32, 1–28.

Ballhaus, C. & Glikson, A.Y. (1995). The petrology of layered mafic-ultramafic intrusions in the Giles Complex, western Musgrave block, central Australia. *AGSO Journal of Australian Geology and Geophysics*, 16, 69–89.

Clarke, G.L., Buick, I.S., Glikson, A.Y. & Stewart, A.J. (1995b). Structural and pressure-temperature evolution of host rocks of the Giles Complex, western Musgrave Block, central Australia: evidence for multiple high-pressure events. *AGSO Journal of Australian Geology and Geophysics*, 16, 127–146.

Coleman, P. (2009). *Intracontinental orogenesis in the heart of Australia: structure, provenance and tectonic significance of the Bentley Supergroup, western Musgrave Block, Western Australia*: Geological Survey of Western Australia, Record 2009/23, 48p.

Donnellan, N., Camacho, A., Maas, R. & Price, R.C. (2019). Mantle upwelling or plume activity on the periphery of the Warakurna LIP: evidence from the geochemistry and petrogenesis of the Alcurra Dolerite in the eastern Musgrave Province. *Journal of Petrology*, 60, 301-327.

Dutch R.A., Werner M.X., Krapf C.B.E. & Rusak T. (2013). *Geology of the TIEYON 1:100 000 map sheet (5645)*, Report Book 2013/00011. Geological Survey of South Australia. Department for Manufacturing, Innovation, Trade, Resources and Energy, South Australia, Adelaide.

Edgoose, C.J., Scrimgeour, I.R. & Close, D.F. (2004). *Geology of the Musgrave Block, Northern Territory.* Northern Territory Geological Survey, Report 15, 48p.

Evins, P.M., Smithies, R.H., Howard, H.M., Kirkland, C.L., Wingate, M.T.D. & Bodorkos, S. (2010b). Devil in the detail: the 1150–1000 Ma magmatic and structural evolution of the Ngaanyatjarra Rift, west Musgrave Province, Central Australia. *Precambrian Research*, 183, 572–588.

Glikson, A.Y. (editor) (1995). *The Giles mafic-ultramafic complex and environs, western Musgrave Block, central Australia.* Thematic issue: AGSO Journal of Geology and Geophysics, 16, no. 1–2, 193p.

Glikson, A.Y., Stewart, A.T., Ballhaus, G.L., Clarke, G.L., Feeken, E.H.T., Level, J.H., Sheraton, J.W. & Sun, S-S. (1996). *Geology of the western Musgrave Block, central Australia, with*

reference to the mafic-ultramafic Giles Complex. Australian Geological Survey Organisation, Bulletin 239, 206p.

Godel, B., Seat, Z., Maier, W.D. & Barnes, S-J. (2011). The Nebo–Babel Ni-Cu-PGE sulfide deposit (West Musgrave Block, Australia): part 2 — constraints on parental magma and processes, with implications for mineral exploration. *Economic Geology*, 106, 557–584.

Goode, A.D.T. (1970). *The petrology and structure of the Kalka and Ewarara layered basic intrusions, Giles Complex, central Australia.* The University of Adelaide, Adelaide, PhD thesis (unpublished).

Goode, A.D.T. (1976a). Small scale primary cumulus igneous layering in the Kalka layered intrusion, Giles Complex, central Australia. *Journal of Petrology*, 17, 379–397.

Goode, A.D.T. (1976b). Sedimentary structures and magma current velocities in the Kalka layered intrusion, central Australia. *Journal of Petrology*, 17, 546–558.

Goode, A.D.T. (1977a). Vertical igneous layering in the Ewarara layered intrusion, central Australia. *Geological Magazine*, 114, 215–218.

Goode, A.D.T. (1977b). Flotation and remelting of plagioclase in the Kalka Intrusion, central Australia: petrological implications for anorthosite genesis. *Earth and Planetary Science Letters*, 34, 375–380.

Goode, A.D.T. (1977c). Intercumulus igneous layering in the Kalka layered intrusion, central Australia. *Geological Magazine*, 114, 215–218.

Goode, A.D.T. (1978). High temperature, high strain rate deformation in the lower crustal Kalka Intrusion, central Australia. *Contributions to Mineralogy and Petrology*, 66, 137–148.

Goode, A.D.T. (2002). The Western Musgrave Block – Australia: Data Metallogenica, District Overview. 42p.

Goode, A.D.T. & Krieg, G.W. (1967). The geology of Ewarara Intrusion, Giles Complex, central Australia. *Journal of the Geological Society of Australia*, 14, 185–194.

Goode, A.D.T. & Moore, A.C. (1975). High pressure crystallisation of the Ewarara, Kalka and Gosse Pile intrusions, Giles Complex, central Australia. *Contributions to Mineralogy and Petrology*, 51, 77–97.

764 Goscombe, B., Czarnota, K., Lawson, C., Everard, J.L., Skirrow, R.G. & Blewett, R. (2020).
765 *Metamorphic evolution of Australia*. Exploring for the future, extended abstracts,
766 Geoscience Australia.

767 Gray, C.M. & Goode, A.D.T. (1989). The Kalka layered intrusion, central Australia: a
768 strontium isotopic history of contamination and magma dynamics. *Contributions to*
769 *Mineralogy and Petrology*, 103, 35–43.

770 Gum, J. & Constable, S. (2003). *Mann Bedrock Drilling Program. South Australia*. Department
771 of Primary Industries and Resources. Report Book, 2003/20.

772 Hollocher K. (2004). *CIPW Norm Calculation Program*. Geology Department, Union College.

773 Howard H.M., Smithies R.H., Kirkland C.L., Kelsey D.E., Aitken A., Wingate M.T.D., Quentin
774 de Gromard R., Spaggiari C.V. & Maier, W.D. (2015). The burning heart — The Proterozoic
775 geology and geological evolution of the west Musgrave Region, central Australia. *Gondwana*
776 *Research*, 27, 64-94

777 Howard, H.M., Quentin de Gromard, R., Smithies, R.H. & Haines, P.W. (2020). Giles Event
778 (MGE): Geological Survey of Western Australia, WA Geology Online, Explanatory Notes
779 extract, viewed 03 November 2022. www.dmp.wa.gov.au/ens

780 Jagodzinski E.A. & Dutch R.A. (2013). *SHRIMP U-Pb Geochronology of the Tieyon (5645)*
781 *1:100 000 mapsheet,* Report Book 2013/00006, Department for Manufacturing, Innovation,
782 Trade, Resources and Energy, South Australia, Adelaide

783 Kelsey, D.E., Hand, M., Evins, P., Clark, C. & Smithies, H. (2009). High temperature, high
784 geothermal gradient metamorphism in the Musgrave Province, central Australia: potential
785 constraints on tectonic setting. In N.E. Timms, J. Foden, K. Evans and C. Clark (Eds.). *Biennial*
786 *conference of the Specialist Group for Geochemistry, Mineralogy and Petrology, Kangaroo*
787 *Island November 2009.* Geological Society of Australia Abstracts No. 96, p. 28.

788 Kelsey, D.E., Hand, M., Smithies, H., Evins, P., Clark, C. & Kirkland, C.L. (2010). *What is the*
789 *tectonic setting of long-lived Grenvillian-aged ultrahigh temperature, high geothermal*
790 *gradient metamorphism in the Musgrave Province, central Australia?* Geological Society of
791 America, Abstracts with Programs, 42(5), p. 516.

Kirkland, C.L., Smithies, R.H., Woodhouse, A.J., Howard, H.M., Wingate, M.T.D., Belousova, E.A., Cliff, J.B., Murphy, R.C. & Spaggiari, C.V. (2013). Constraints and deception in the isotopic record; the crustal evolution of the west Musgrave Province, central Australia. *Gondwana Research*, 23, 759–781

Maier, W.D., Barnes, S-J. & Groves, D.I. (2013b). The Bushveld Complex, South Africa: Formation of platinum–palladium, chrome and vanadium- rich layers via hydrodynamic sorting of a mobilized cumulate slurry in a large, relatively slowly cooling, subsiding magma chamber. *Mineralium Deposita*, 48, 1–56.

Maier, W.D., Howard, H.M., Smithies, R.H., Yang, S.H., Barnes, S.J., O'Brien, H., Huhma, H. & Gardoll, S. (2015). Magmatic ore deposits in mafic–ultramafic intrusions of the Giles Event, Western Australia. *Ore Geology Reviews*, 71, 405-436.

Major, R. B. & Conor, C. H. H. (1993). The Musgrave Block. In: J.F. Drexel, W.P. Preiss and A.j. Parker (Eds.), *The Geology of South Australia, Vol.1. The Precambrian* (pp. 156-167). Geological Survey of South Australia. Bulletin 54.

Nesbitt, R.W., Goode, A.D.T., Moore, A.C. & Hopwood, T.P. (1970). *The Giles Complex, central Australia: a stratified sequence of mafic and ultramafic intrusions* (pp. 547–564). Special Publications of the Geological Society of South Africa, 1.

Nesbitt, R.W. & Talbot, J.L. (1966). The layered basic and ultrabasic intrusives of the Giles Complex, central Australia. *Contributions to Mineralogy and Petrology*, 13, 1–11.

Pollett, A., Thiel, S., Bendall, B., Raimondo, T. & Hand, M. (2019). Mapping the Gawler Craton–Musgrave Province interface using integrated heat flow and magnetotellurics. *Tectonophysics*, 756, 43-56.

Quentin de Gromard, R. & Howard, H.M. (2019). Warlawurru Supersuite: Geological Survey of Western Australia, WA Geology Online, Explanatory Notes extract, viewed 03 November 2022, www.dmp.wa.gov.au/ens>

Quentin de Gromard, R., Howard, H.M. & Smithies, R.H. (2020). Petermann Orogeny (PE): Geological Survey of Western Australia, WA Geology Online, Explanatory Notes extract, viewed 03 November 2022, www.dmp.wa.gov.au/ens>

820 Scrimgeour, I.R. & Close, D.F. (1999). Regional high pressure metamorphism during
821 intracratonic deformation: the Petermann orogeny, central Australia. *Journal of*
822 *Metamorphic Geology*, 17, 557–572.

823 Seat, Z. (2008). *Geology, petrology, mineral and whole-rock chemistry, stable and radiogenic*
824 *isotope systematics and Ni–Cu–PGE mineralisation of the Nebo–Babel intrusion, west*
825 *Musgrave, Western Australia*: The University of Western Australia, Perth, PhD thesis
826 (unpublished).

827 Seat, Z., Beresford, S.W., Grguric, B.A., Gee, M.A. & Grassineau, N.V. (2009). Reevaluation of
828 the role of external sulfur addition in the genesis of Ni–Cu–PGE deposits: evidence from the
829 Nebo–Babel Ni–Cu–PGE deposit: West Musgrave, Western Australia. *Economic Geology*,
830 104, 521–538.

831 Seat, Z., Beresford, S.W., Grguric, B.A., Waugh, R.S., Hronsky, J.M.A., Gee, M.M.A., Groves,
832 D.I. & Mathison, C.I. (2007). Architecture and emplacement of the Nebo–Babel gabbro-
833 norite-hosted magmatic Ni–Cu–PGE sulfide deposit, West Musgrave, Western Australia.
834 *Mineralium Deposita*, 42, 551–582.

835 Sheraton, J.W. & Sun, S-s. (1995). Geochemistry and origin of felsic igneous rocks of the
836 western Musgrave Block. *AGSO Journal of Australian Geology and Geophysics*, 16, 107–125.

837 Smithies, R.H., Howard, H.M., Evins, P.M., Kirkland, C.L., Bodorkos, S. & Wingate, M.T.D.
838 (2009). *The west Musgrave Complex — some new geological insights from recent mapping,*
839 *geochronology, and geochemical studies*: Geological Survey of Western Australia, Record
840 2008/19, 20p.

841 Smithies, R.H., Howard, H.M., Evins, P.M., Kirkland, C.L., Kelsey, D.E., Hand, M., Wingate,
842 M.T.D., Collins, A.S., Belousova, E. & Allchurch, S. (2010). *Geochemistry, geochronology and*
843 *petrogenesis of Mesoproterozoic felsic rocks in the western Musgrave Province of central*
844 *Australia, and implication for the Mesoproterozoic tectonic evolution of the region*:
845 Geological Survey of Western Australia, Report 106, 73p.

846 Smithies, R.H., Howard, H.M., Evins, P.M., Kirkland, C.L., Kelsey, D.E., Hand, M., Wingate,
847 M.T.D., Collins, A.S. & Belousova, E. (2011). Mesoproterozoic high temperature granite

848 magmatism, crust–mantle interaction and the intracontinental evolution of the Musgrave
849 Province. *Journal of Petrology*, doi:10.1093/petrology/egr010.

850 Smithies, R.H., Howard, H.M., Kirkland, C.L., Werner, M., Medlin, C.C., Wingate, M.T.D. &
851 Cliff, J.B. (2013). *Geochemical evolution of rhyolites of the Talbot Sub-basin and associated*
852 *felsic units of the Warakurna Supersuite.* Geological Survey of Western Australia, Report
853 118, 74p.

854 Smithies, R.H., Kirkland, C.L., Korhonen, F.J., Aitken, A.R.A., Howard, H.M., Maier, W.D.,
855 Wingate, M.T.D., Quentin de Gromard, R. & Gessner, K. (2015). The Mesoproterozoic
856 thermal evolution of the Musgrave Province in central Australia – Plume vs. the geological
857 record. *Gondwana Research*, 27, 64-94

858 Smithies, R.H., Howard, H.M., Kirkland, C.L., Korhonen, F.J., Medlin, C.C., Maier, W.D., De
859 Gromard, R.Q. & Wingate, M.T.D. (2015). Piggy-back supervolcanoes—long-lived,
860 voluminous, juvenile rhyolite volcanism in Mesoproterozoic central Australia. *Journal of*
861 *Petrology*, 56(4), 735-763.

862 Smits, R. G., Collins W.J., Hand, M., Dutch, R. & Payne J., (2014). A Proterozoic Wilson cycle
863 identified by Hf isotopes in central Australia: Implications for the assembly of Proterozoic
864 Australia and Rodinia. *Geology* 42, 231-234

865 Sprigg, R.C. & Wilson, R.B. (1959). The Musgrave mountain belt in South Australia.
866 *Geologische Rundschau*, 47, 531–542.

867 Stewart, A.J. (1995). Resolution of conflicting structures and deformation history of the
868 Mount Aloysius granulite massif, western Musgrave Block, central Australia. *AGSO Journal of*
869 *Australian Geology and Geophysics*, 16, 91–105.

870 Sun, S.-s. & McDonough, W.F. (1989). Chemical and isotopic systematics of oceanic basalts:
871 implications for mantle composition and processes. In AD Saunders and MJ Norry (Eds.),
872 *Magmatism in the Ocean Basins (p*p. 313–345). Geological Society, Special Publication, 42.

873 Sun, S-S., Sheraton, J.W., Glikson, A.Y. & Stewart, A.J. (1996). A major magmatic event
874 during 1050–1080 Ma in central Australia, and an emplacement age for the Giles Complex.
875 *AGSO Journal of Australian Geology and Geophysics*, 24, 13–15.

Tucker, N.M., Hand, M., Kelsey D.E. & Dutch R.A. (2015). A duality of timescales: Short-lived ultrahigh temperature metamorphism preserving a long-lived monazite growth history in the Grenvillian Musgrave–Albany–Fraser Orogen. *Precambrian Research*, 264, 204-234

Wade, B.P. (2006). *Unravelling the tectonic framework of the Musgrave Province, central Australia*: The University of Adelaide, Adelaide, PhD thesis (unpublished).

Wade, B. P., Barovich, K. M., Hand, M., Scrimgeour, I. R. & Close, D. F. (2006). Evidence for Early Mesoproterozoic Arc Magmatism in the Musgrave Block, Central Australia: Implications for Proterozoic Crustal Growth and Tectonic Reconstructions of Australia. *The Journal of Geology*, 114, 43-63.

White, R.W., Clarke, G.L. & Nelson, D.R. (1999). SHRIMP U–Pb zircon dating of Grenville-age events in the western part of the Musgrave Block, central Australia. *Journal of Metamorphic Geology*, 17, 465–481.

Wingate, M.T.D. & Evans, D.A.D. (2003). Palaeomagnetic constraints on the Proterozoic tectonic evolution of Australia. In M. Yoshida, B.F. Windley, and S. Dasgupta (Eds), *Proterozoic East Gondwana: Supercontinent Assembly and Breakup* (pp. 77-91). Geological Society, London, Special Publications, 206.

Wingate, M.T.D., Pirajno, F. & Morris, P.A. (2004). Warakurna large igneous province: a new Mesoproterozoic large igneous province in west-central Australia. *Geology*, 32, 105–108.

Zhao, J-X., McCulloch, M.T. & Korsch, R.J. (1994). Characterisation of a plume-related ~800 Ma magmatic event and its implications for basin formation in central-southern Australia. *Earth and Planetary Science Letters*, 121, 349–367.

Figure Captions

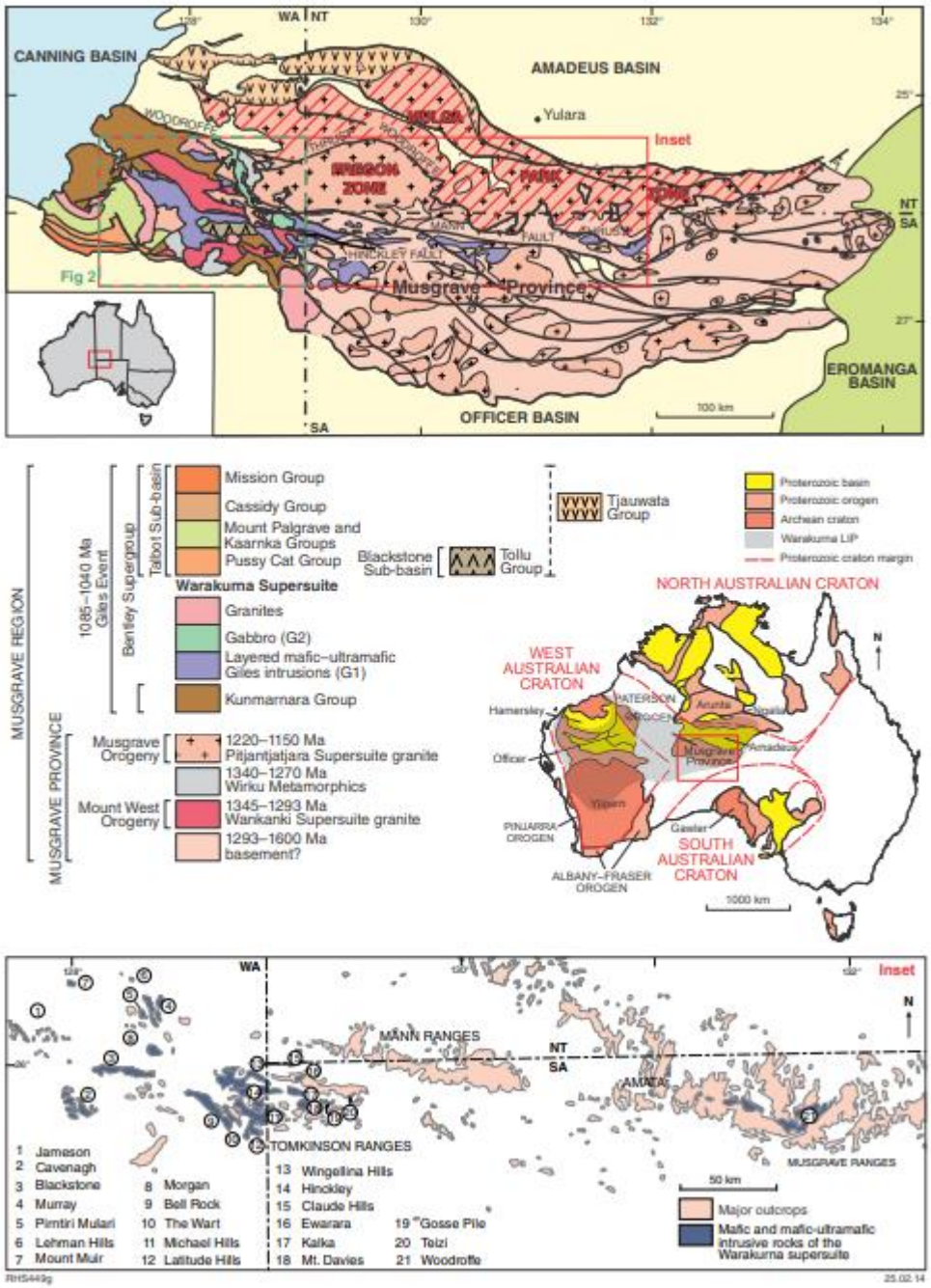

914

915 Fig. 1a-c: Simplified geological map of the Musgrave Province, with mafic–ultramafic

916 intrusions highlighted in bottom panel (figure from Maier et al. 2015).

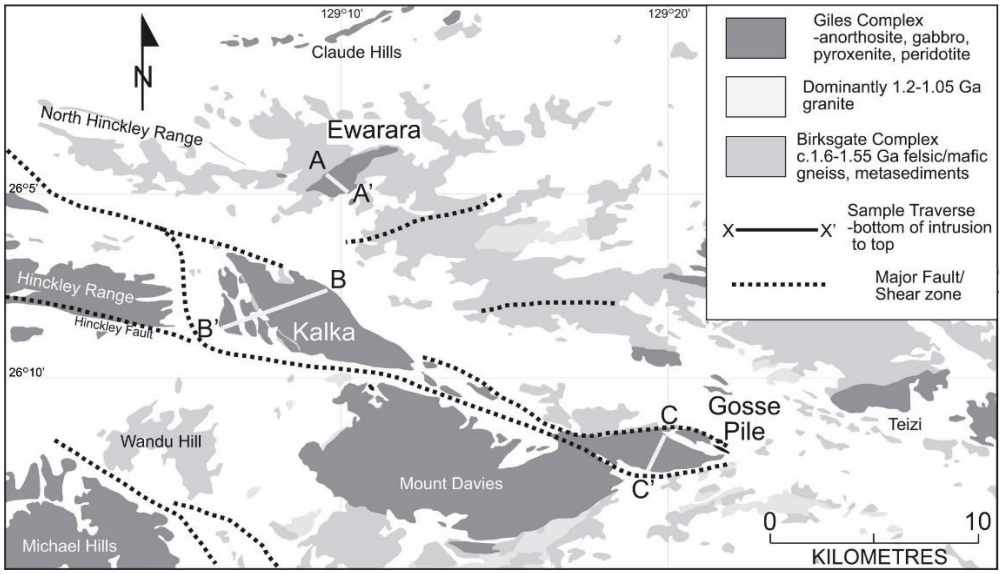

917

918 Fig. 2: Outcrop map with sample traverses of the studied intrusions.

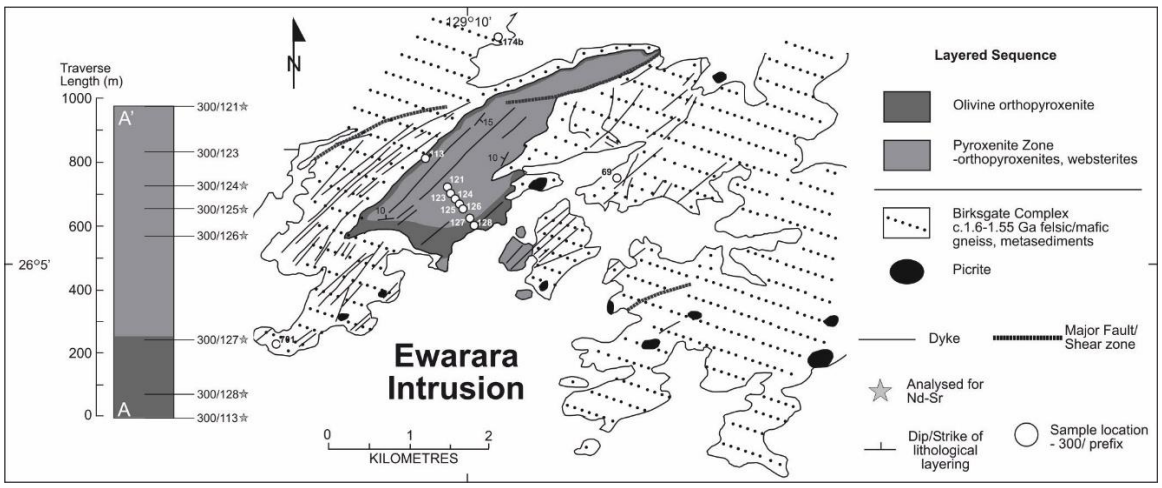

919

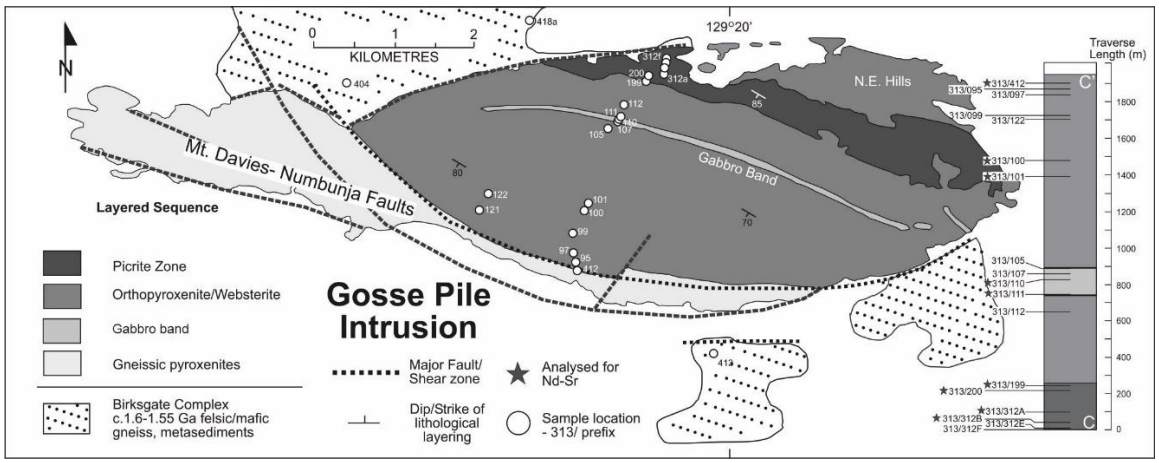

920

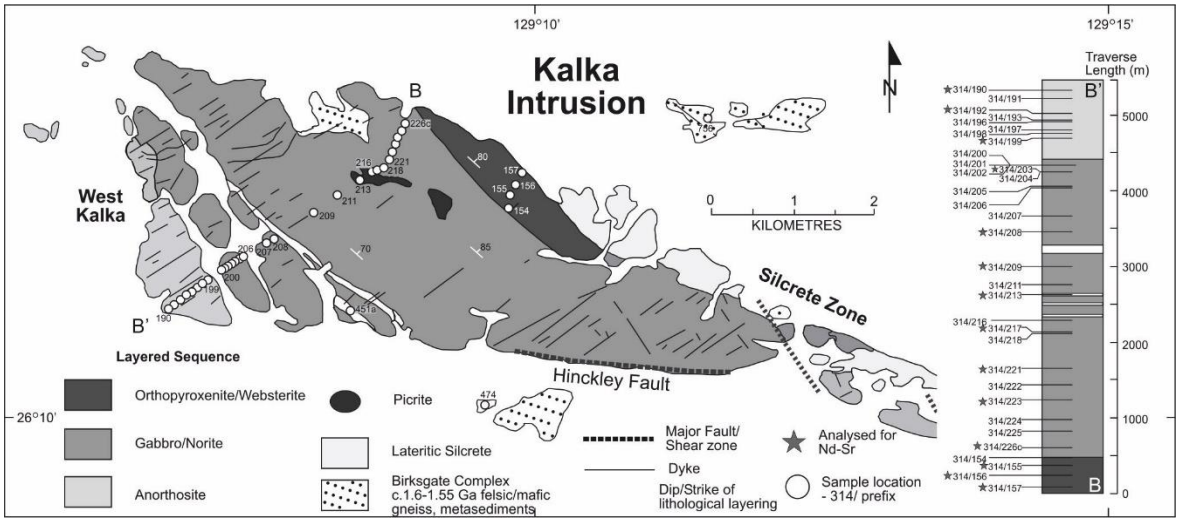

921

922 Fig. 3a: Generalised map of Ewarara intrusion displaying sample locations (after Goode and
923 Krieg 1965). b: Generalised map of Gosse Pile intrusion displaying sample locations (after
924 Moore 1970). c: Generalised geological map of Kalka intrusion with sample locations (after
925 Goode 1970).

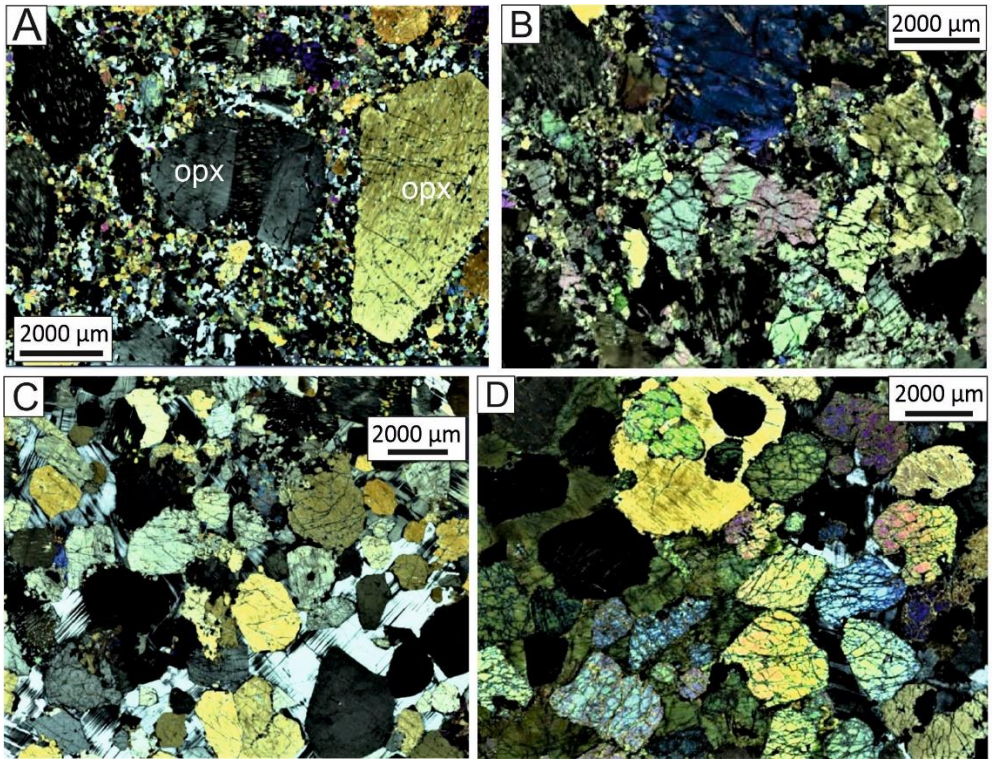

926

927 Fig. 4: Selected ultramafic lithologies from the studied intrusions illustrating variability in
928 degree of deformation modal proportions. (A) Orthopyroxenite showing mosaic texture and
929 kink banding, Kalka Pyroxenite Zone, sample 157, 90 mab, (b) Peridotite showing highly
930 irregular grain boundaries, Ewarara, sample 300-128, 80 mab, (C) Pyroxenite showing
931 aubhedral pyroxene morphologies and intertitial plagioclase, Gosse Pile, sample 313-312b,
932 50 mab, (D) Peridotite showing subhedral grain morphologies, Gosse Pile, sample 313-199,
933 250 mab.

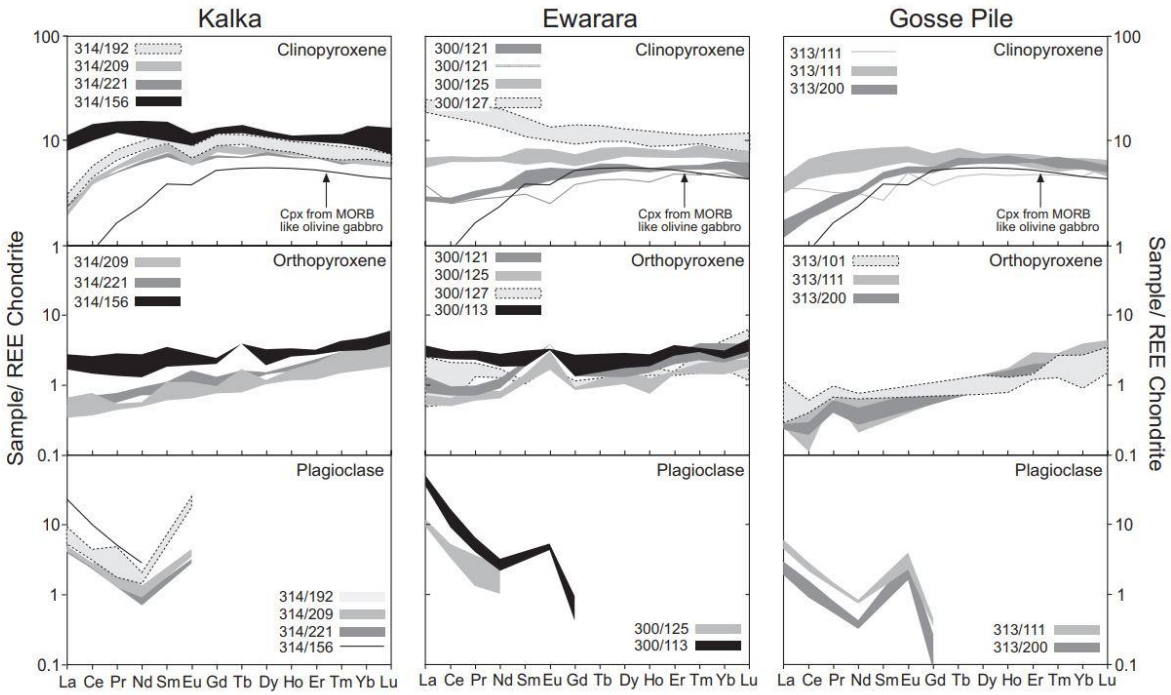

934

935 Fig. 5: Laser ablation ICP-MS REE data for orthopyroxene, clinopyroxene and plagioclase
936 from Kalka, Ewarara and Gosse Pile. Note that at Kalka and Ewarara REE are enriched in the
937 basal rocks, whereas at Gosse Pile the interpreted basal portion is REE depleted.

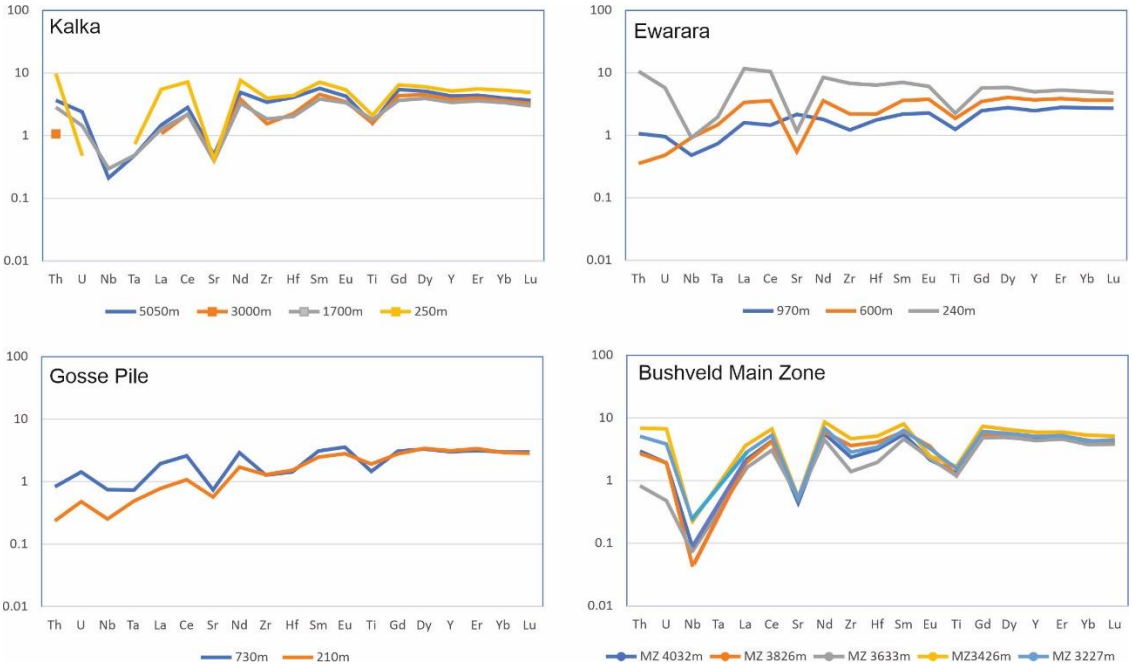

938

939 Fig. 6: Trace element data for clinopyroxene from Kalka, Ewarara and Gosse Pile. Data for
940 the Main Zone of the Bushveld Complex are shown for comparison (from Yang et al., 2020).
941 Note that at Kalka and Ewarara, the highest incompatible trace element contents and most
942 pronounced negative Nb-Ta anomaly occur in the lowermost sample. See text for further
943 discussion.

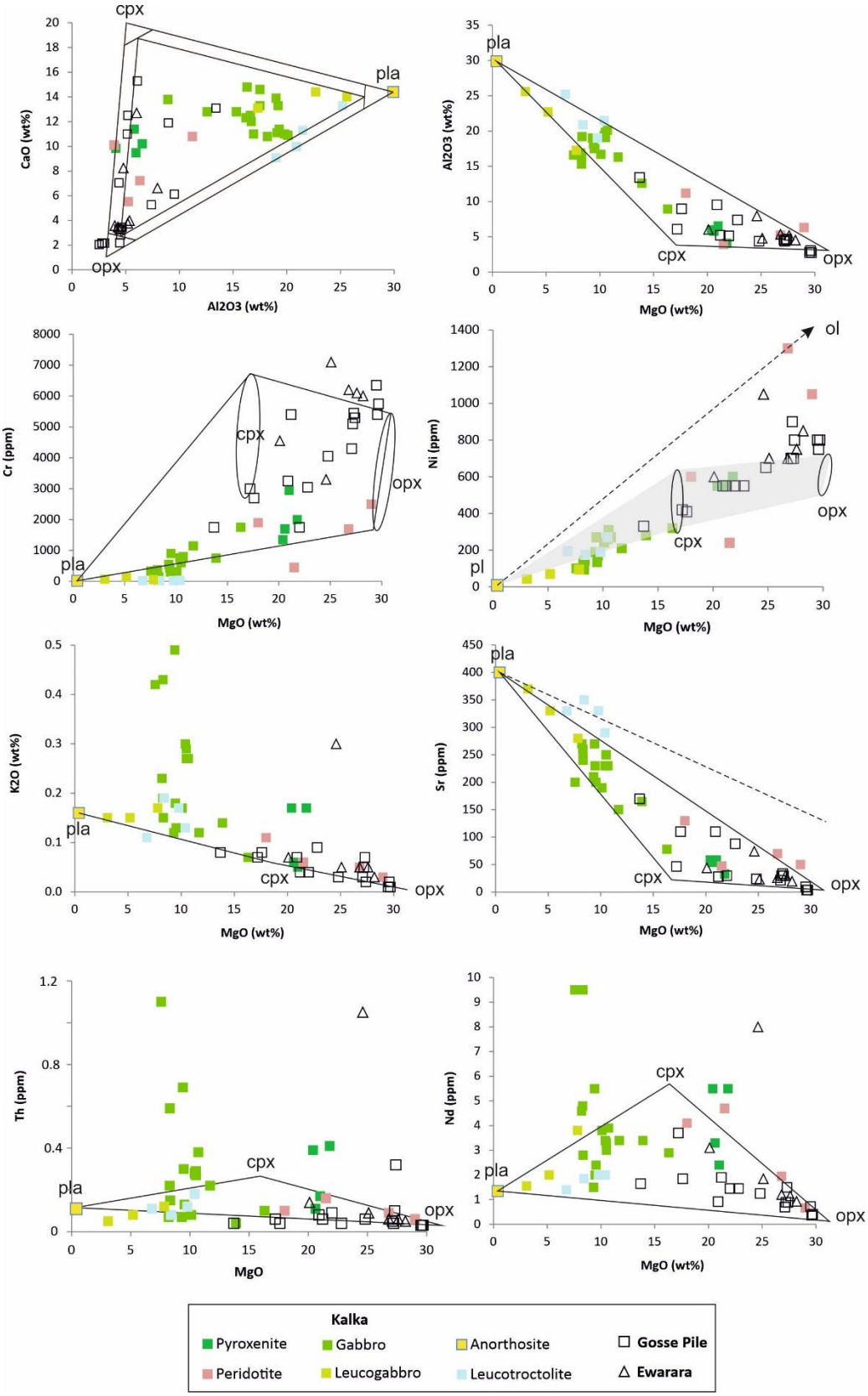

944

945 Fig. 7: Binary variation diagrams of lithophile major and trace elements. (A) CaO vs Al2O3,
946 (B) Al2O3 vs MgO, (C) Cr vs MgO, (D) Ni vs MgO, (E) K2O vs MgO, (F) Sr vs MgO, (G) Th vs
947 MgO, and (H) Nb vs MgO.

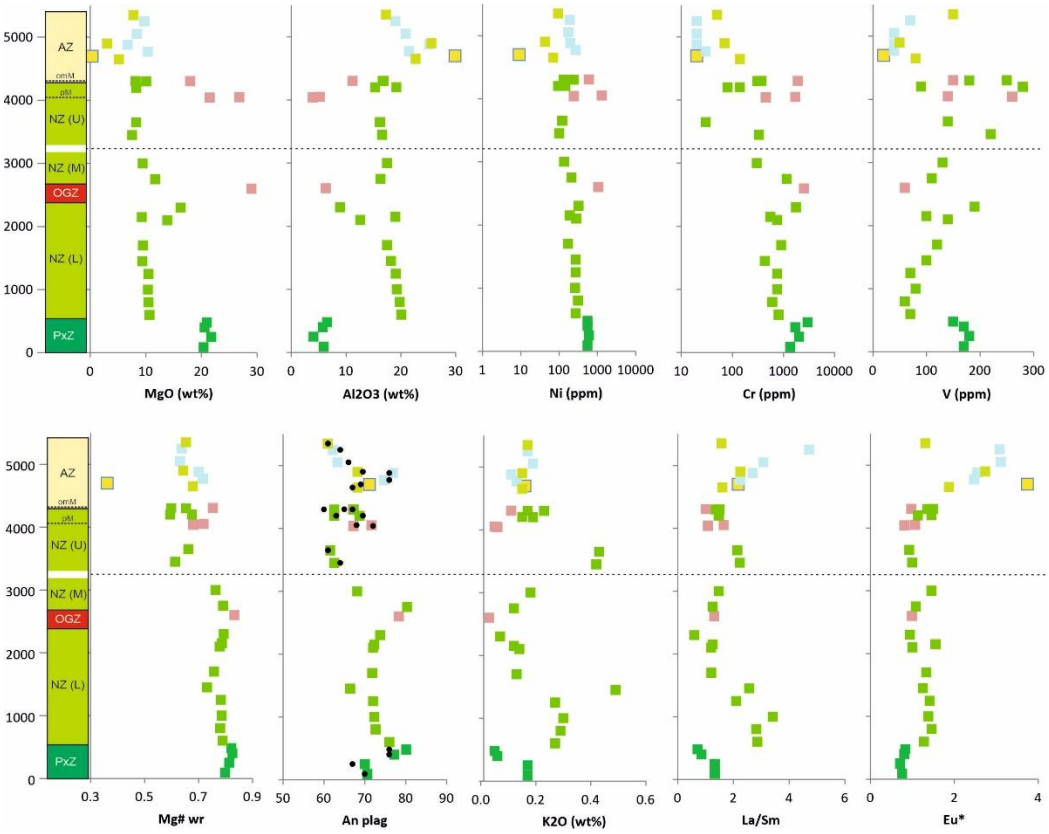

Fig. 8: Lithophile major and trace element compositional variation at Kalka. PxZ=Pyroxenite zone, GZL,M,U=Gabbronorite zone (lower, middle, upper), OGZ=Olivine gabbro zone, AZ = Anorthosite Zone. pm=peridotite member, omm=olivine magnetite member. Data on An content of plagioclase represent model calculated using the CIPW program of Hollocher (2004). Small black dots in An column represent data of Gray and Goode (1983).

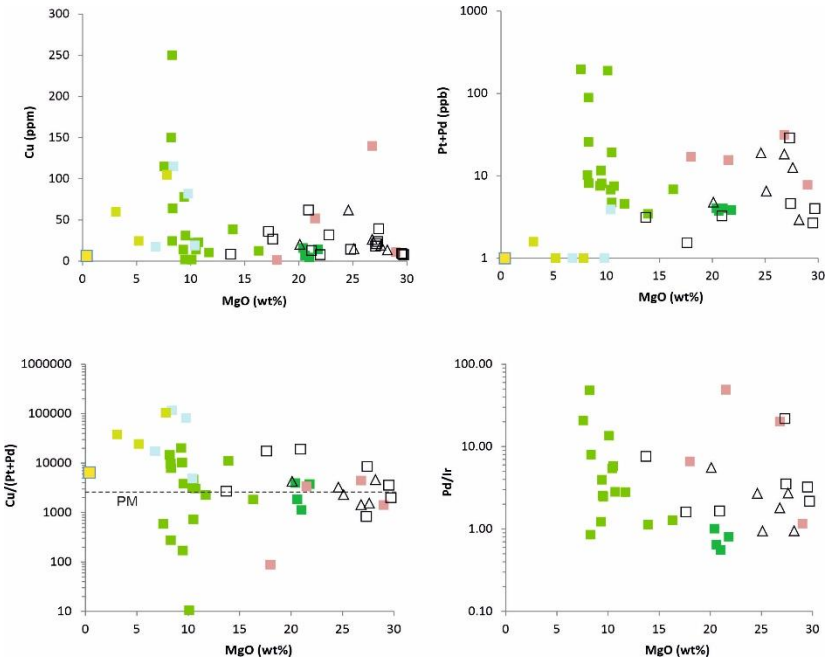

Fig. 9: Diagrams illustrating variation in chalcophile metals and metal ratios in analysed intrusions. (A) Cu vs MgO, (B) Pt+Pd vs MgO, (D) Cu/(Pt+Pd) vs MgO, (D) Pd/Ir vs MgO.

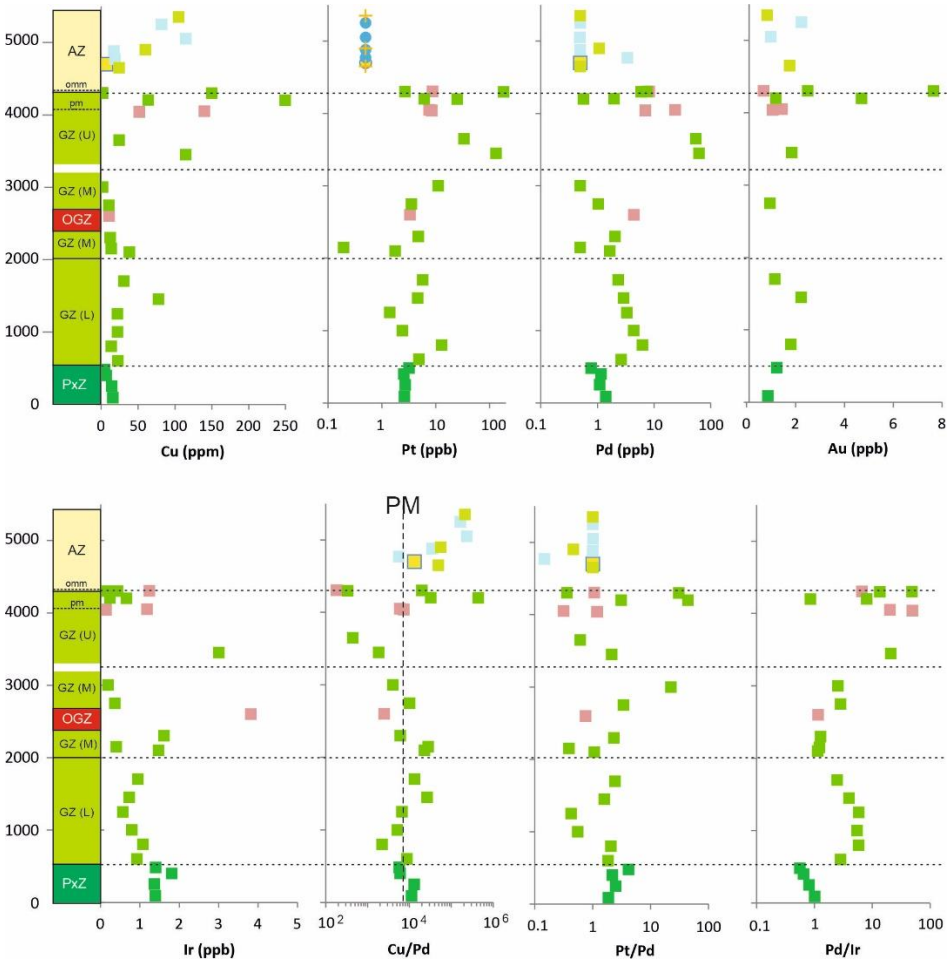

957

958 Fig. 10: Chalcophile element concentrations and element ratios plotted vs stratigraphic
959 height at Kalka. PxZ=Pyroxenite zone, GZL,M,U=Gabbronorite zone (lower, middle, upper),
960 OGZ=Olivine gabbro zone, AZ = Anorthosite Zone. pm=peridotite member, omm=olivine
961 magnetite member.

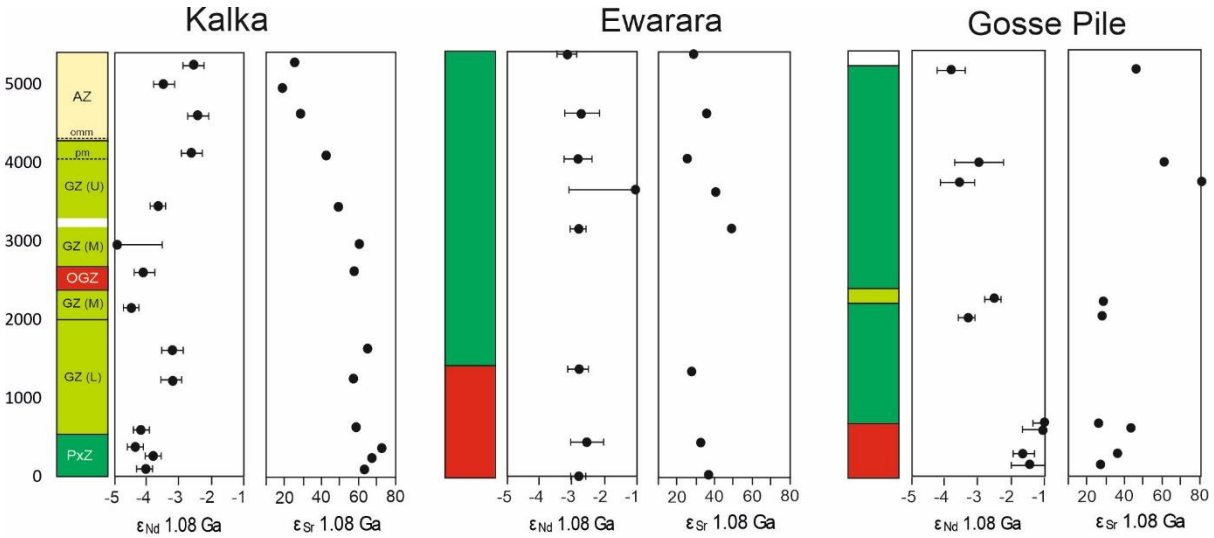

962

963 Fig. 11: Variation in εNd and εSr plotted vs stratigraphic height at (A) Kalka, (B) Ewarara, and
964 (C) Gosse Pile. Note that Kalka shows a trend towards unenriched isotopic signature,
965 whereas Ewarara lacks a clear trend and Gosse Pile shows a trend towards a more enriched
966 signature with height. See text for further discussion.

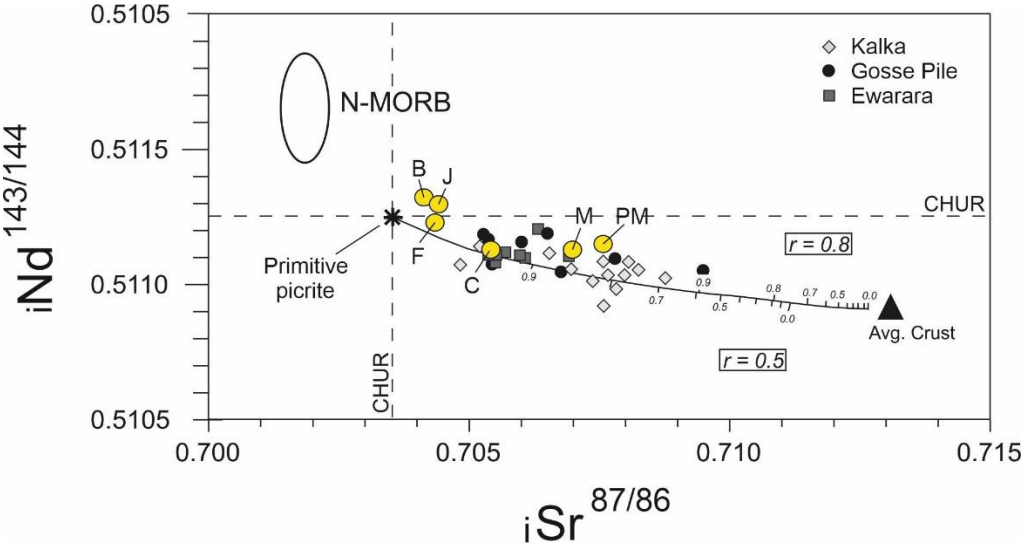

Fig. 12: Model of crustal contamination of Giles intrusions, assuming AFC at R=0.8 and 0.5. Average crust is based on the average composition of several host rock samples collected near the intrusions. Average values of Western Australian intrusions are from Maier et al. (2015). Primitive picritic basalt composition from Arndt et al. (1998). PM=Pirntirri Mulari, M=Morgan, B=Blackstone-Bell Rock, J=Jameson, F=Finlayson, C=Cavenagh.

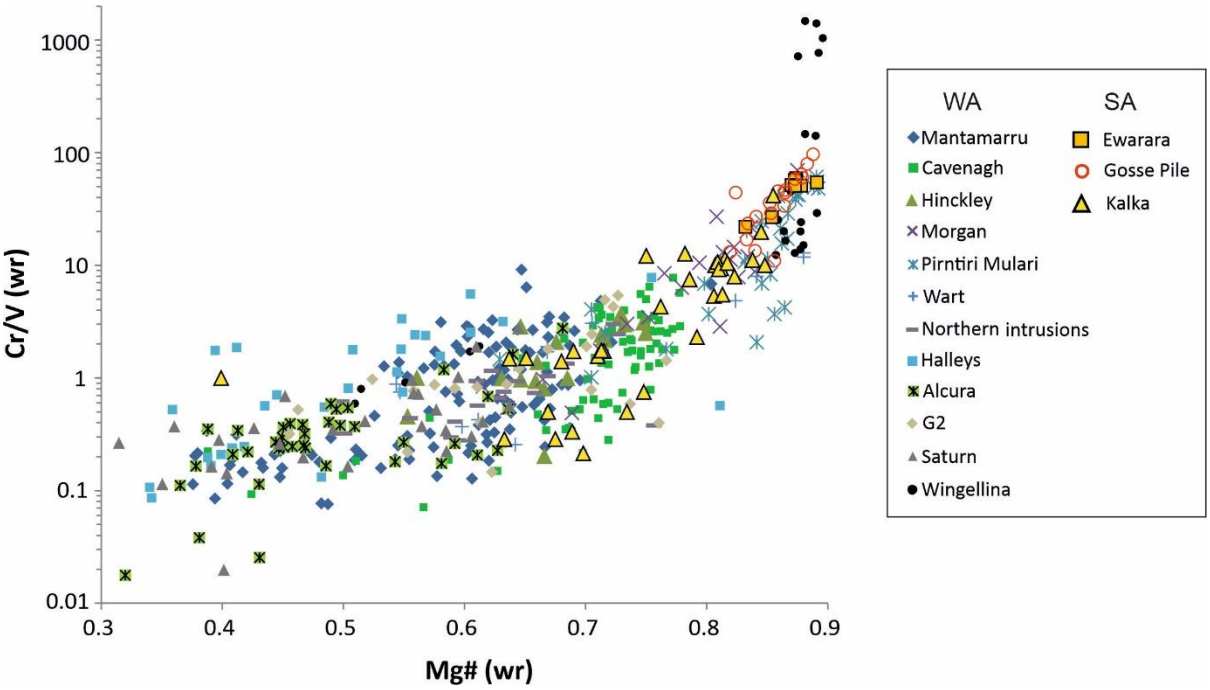

Fig. 13. Binary variation diagram of Cr/V vs MgO for Musgrave intrusives. Note that the South Australian intrusions studied here have amongst the highest MgO and Cr/V attesting to their unevolved character.

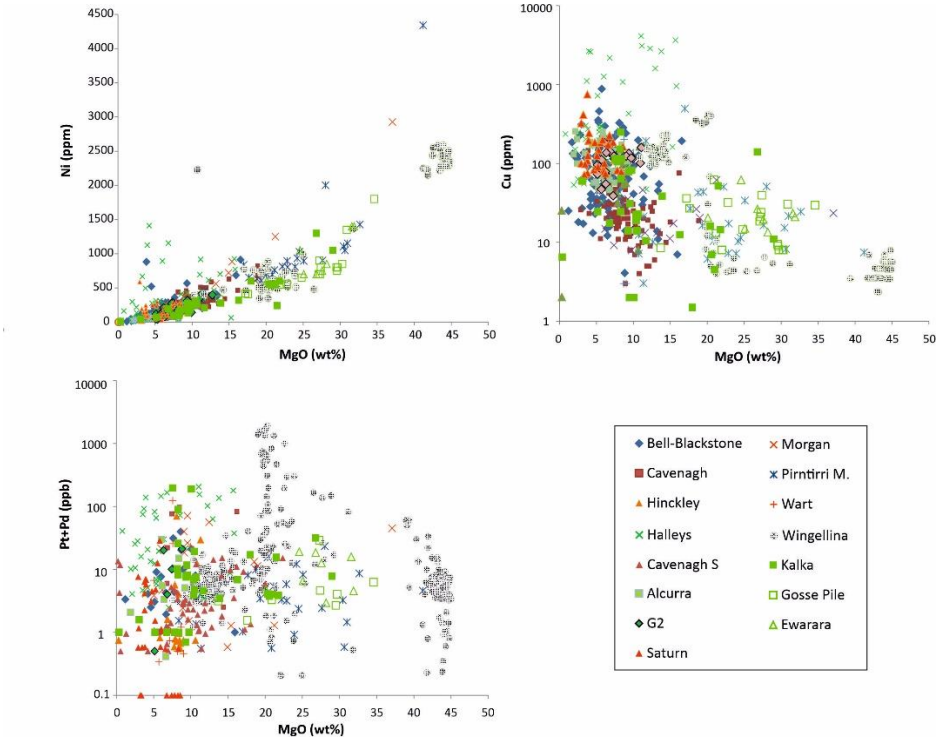

977

978 Fig. 14: Binary variation diagrams plotting Giles intrusions vs MgO of (a) Ni, (b) Cu and (c)
979 Pt+Pd. Note that Ewarara and Gosse Pile broadly overlap with Pirntirri Mulari and Wingellina
980 in terms of Ni, Cu, and PGE, but they lack the dunites and PGE enrichment of Wingellina
981 Hills.

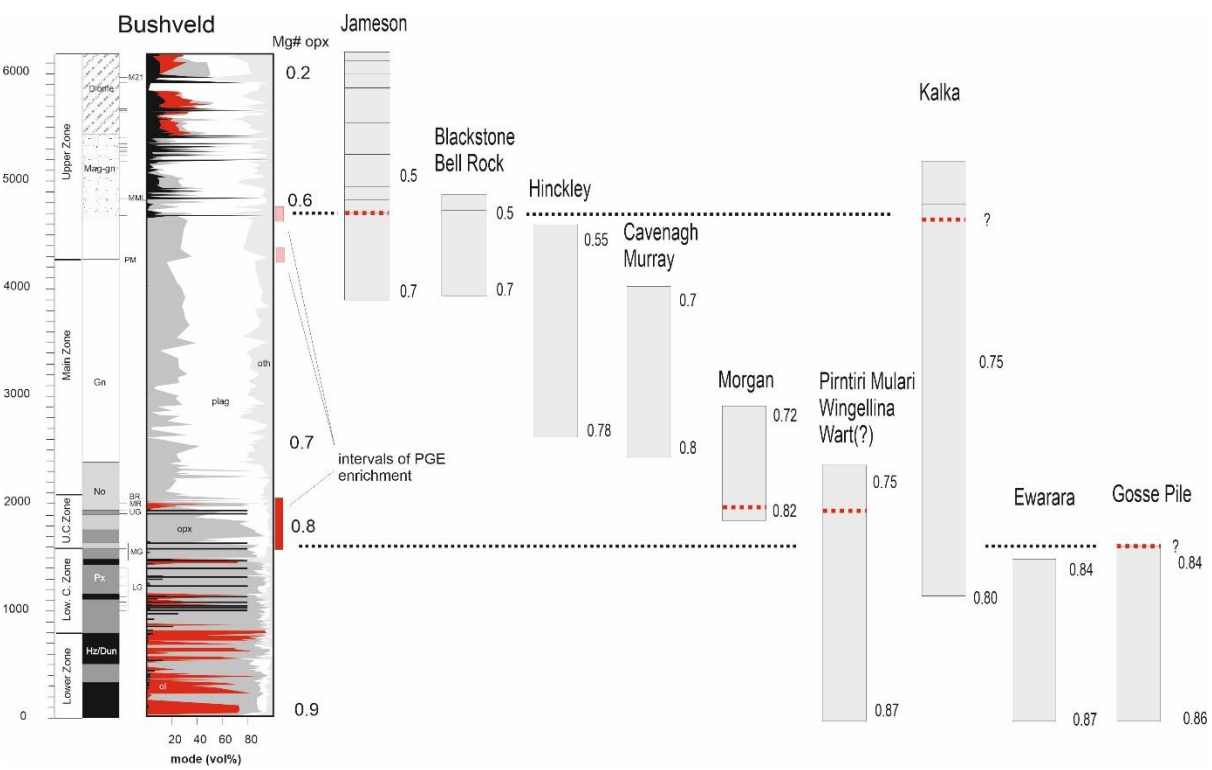

982

983 Fig. 15: Stratigraphic comparison of Giles intrusions with Bushveld Complex. Low. C. Zone =
984 Lower Critical Zone. U.C. Zone = Upper Critical Zone. Red stippled line indicates approximate
985 position of (postulated) main PGE reef horizon. Red-pink bars to right of Bushveld indicate
986 key mineralised intervals. Figure modified after Maier et al. (2015).